Air-sea CO_2 fluxes in the East China Sea based on multiple-year underway observations

X.-H. Guo[1], W.-D. Zhai[1, 2], M.-H, Dai[1, *], C. Zhang[1], Y. Bai[3], Y. Xu[1], Q. Li[1], G.-Z. Wang[1]

[1] {State Key Laboratory of Marine Environmental Science, Xiamen University, Xiamen 361102, China

[2] {National Environmental Monitoring Center, Dalian 116023, China}

[3] {State Key Laboratory of Satellite Ocean Environment Dynamics, Second Institute of Oceanography, State Oceanic Administration, Hangzhou 310012, China}

Correspondence to: M.-H. Dai (mdai@xmu.edu.cn)

Abstract

This study reports thus far a most comprehensive dataset of surface seawater pCO_2 (partial pressure of CO_2) and the associated air-sea CO_2 fluxes in a major ocean margin, the East China Sea (ECS) based on 24 surveys conducted in 2006 to 2011. We showed highly dynamic spatial variability of sea surface pCO_2 in the ECS except in winter when it ranged in a narrow band of 330 to 360 μatm. In this context, we categorized the ECS into five different domains featured with different physics and biogeochemistry to better characterize the seasonality of the pCO_2 dynamics and to better constrain the CO_2 flux. The five domains are (I) the outer Changjiang estuary and Changjiang plume, (II) the Zhejiang-Fujian coast, (III) the northern ECS shelf, (IV) the middle ECS shelf, and (V) the southern ECS shelf. In spring and summer, pCO_2 off the Changjiang estuary was as low as <100 μatm, while it was up to >400 μatm in fall. pCO_2 along the Zhejiang-Fujian coast was low in spring, summer and winter (300 to 350 μatm) but was relatively high in fall (>350 μatm). In the northern ECS shelf, pCO_2 in summer and fall was >340 μatm in most areas, higher than in winter and spring. In the middle and southern ECS shelf, pCO_2 in summer ranged from 380 to 400 μatm, which was higher than in other seasons (<350 μatm). The area-weighted CO_2 flux in the entire ECS shelf was -10.0±2.0 mmol m^{-2} d^{-1} in winter, -11.7±3.6 mmol m^{-2} d^{-1} in spring, -3.5±4.6 mmol m^{-2} d^{-1} in summer and -2.3±3.1 mmol m^{-2} d^{-1} in fall. It is important to note that the standard deviations in these flux ranges mostly reflect the spatial variation of pCO_2, which differs from the spatial variance nor the bulk uncertainty. Nevertheless, on an annual basis, the average CO_2 influx into the entire ECS shelf was -6.9±4.0 mmol m^{-2} d^{-1}, about twice the global average in ocean margins.

1 Introduction

With the rapid growth of carbon flux measurements during the past decade, our estimation of the coastal ocean air-sea CO_2 fluxes have converged to a reasonably agreeable estimate of about 0.2 to 0.5 Pg C yr^{-1} at a global scale (Borges et al., 2005;

Cai et al., 2006; Chen and Borges, 2009; Chen et al., 2013; Dai et al., 2013; Laruelle et al., 2010; Laruelle et al., 2014) and it is safe to state that the earlier estimate of up to 0.9 to 1.0 Pg C yr^{-1} was an overestimate. Having stated so, it remains, however, challenging to reliably assess the carbon fluxes in individual coastal systems that are often featured by the greatest variations in time and space both in terms of fluxes and their intrinsic controls. Understanding regional fluxes and controls is important both because it would affect global flux estimation, and in order to improve our modeling capability of the coastal ocean carbon cycle. A regional climate model that is particularly relevant to the societal sustainability would need an improved estimate of regional carbon fluxes to resolve its predictability of future changes. Finally, it has been recognized that anthropogenic activities have been increasingly embedded in many coastal oceans so that studying such human perturbation on carbon cycling remains challenging (Chou et al., 2007; Omar et al., 2003).

The East China Sea (ECS) is a shelf system featured with significant terrestrial input from a major world river from the west, the Changjiang (Yangtze River), as well as dynamic exchange at its eastern board with the Kuroshio, a major western ocean boundary current (Chen and Wang, 1999). Located in the temperate zone, the ECS is also characterized by a clear seasonal pattern with warm and productive summer, and cold and less productive winter (Gong et al., 2003; Han et al., 2013). Such a dynamic nature in both physical circulation and biogeochemistry make for large contrasts in different zones within the ECS and thus zonal based assessment is critical to reliably constrain the CO_2 flux in time and space in this important marginal sea.

Prior studies already reveal that the ECS is overall an annual net sink of the atmospheric CO_2 with remarkable seasonal variations (Chou et al., 2009; Chou et al., 2011; Kim et al., 2013; Peng et al., 1999; Shim et al., 2007; Tseng et al., 2011; Tsunogai et al., 1999; Wang et al., 2000; Zhai and Dai, 2009). The ranges of present estimates are -3.3 to -6.5 mmol m^{-2} d^{-1} in spring, -2.4 to -4.8 mmol m^{-2} d^{-1} in summer, 0.4 to 2.9 mmol m^{-2} d^{-1} in fall and -13.7 to -10.4 mmol m^{-2} d^{-1} in winter. However,

these estimates are either based on limited (only one or a few) field surveys (Chou et al., 2009; Chou et al., 2011; Peng et al., 1999; Shim et al., 2007; Tsunogai et al., 1999; Wang et al., 2000) or suffering from spatial limitation (Kim et al., 2013; Shim et al., 2007; Tsunogai et al., 1999; Zhai and Dai, 2009). Tseng et al. (2011) investigate the Changjiang Dilution Water induced CO_2 uptake in summer and obtain an empirical algorithm of surface water pCO_2 (partial pressure of CO_2) with the Changjiang river discharge and sea surface temperature (SST). Subsequently, they extrapolate the empirical algorithm to the entire ECS shelf and the whole year to obtain a significant CO_2 sink of 6.3±1.1 mmol m^{-2} d^{-1} (Tseng et al., 2011). With data from three field surveys conducted in spring, fall and winter added, Tseng et al. (2014) update the annual CO_2 flux in the ECS to be -4.9±1.4 mmol m^{-2} d^{-1} using the similar empirical algorithm method.

In this study, we investigated the air-sea CO_2 fluxes on the entire ECS shelf based on large scale observations during 24 mapping cruises from 2006 to 2011, resolving both spatial coverage and fully seasonal variations. This largest dataset, thus far, allowed for a better constraint of the carbon fluxes in this important ocean margin system. The estimate in an individual survey was based on the gridded average in five physically and biogeochemically distinct domains (Fig. 1), which were then averaged for each season and finally the annual average was calculated.

Domains I and II are essentially in the inner shelf shallower than 50 m, with Domain I being the core area of the outer Changjiang estuary and the near field Changjiang plume in warm seasons, while Domain II is off the Zhejiang-Fujian coast and featured by turbid coastal waters and the Changjiang plume in winter. Domains III, IV and V are all located in the mid- and outer shelf, influenced by the Kuroshio and thus characterized by lower nutrients and warm temperature. The difference is that Domain III is impacted by far field river plume in flood seasons but Domain IV is not (Bai et al., 2014). Domain V is characterized by upwelling off northern Taiwan. Based on the above constraint of seasonal and intra-seasonal variations in five spatially distinct

(five physico-biogeochemical domains) and temporal (seasonal and intra-seasonal) scales, the distribution characteristics of the pCO_2 and the major controls in the ECS were better revealed, and the air-sea CO_2 fluxes were better estimated..

2 Study area

The ECS is one of the major marginal seas located in the western Pacific. The largest freshwater source to the ECS is the Changjiang, which delivers 940 km^3 freshwater annually with the highest discharge in summer (Dai and Trenberth, 2002). The circulation of the ECS is modulated by the East Asian monsoon. The northeast winds in winter last from September to April and the summer monsoon from the southwest is weaker and lasts from July to August. The Changjiang plume flows northeastward in summer but southwestward along the China coastline in winter (Lee and Chao, 2003). The northward flowing Kuroshio follows the isobaths beyond the shelf break at ~200 m (Lee and Chao, 2003; Liu and Gan, 2012). Near the shelf break, there are upwellings centered at the northeast of Taiwan Island and the southwest of Kyushu Island (Lee and Chao, 2003).

The SST in the ECS is low in winter and early spring but high in summer and early fall. The seasonal variation in SST is up to 10 ℃ in the inner shelf and ~5 ℃ in the outer shelf (Gong et al., 2003). In warm seasons, productivity in the ECS is as high as >1 g C m^{-2} d^{-1} (Gong et al., 2003). Changjiang freshwater and the upwelling of the Kuroshio subsurface water are believed to be the major sources of nutrients to the ECS shelf (Chen and Wang, 1999). Regulated by both productivity and temperature, pCO_2 shows strong seasonal variations, typically under-saturated in cold seasons and in productive areas in warm seasons (Chou et al., 2009; Chou et al., 2011; Tseng et al., 2011).

This study covers largely the entire ECS shelf (< 200 m). We categorized the ECS shelf into five distinct domains featured by different physico-biogeochemical characteristics based on the distributions of SST, chlorophyll a (Chl-*a*) concentration and turbidity (Fig. 1). The boundaries, surface areas and characteristics of the five domains are presented in Table 1 and Fig. 1.

Domain I (28.5-33.0 ℃N, 122.0-126.0 ℃E, 191×10^3 km^2) is characterized by high Chl-*a*

(He et al., 2013) and lowest pCO_2 in warm seasons. It covers most of the area within the 50 m isobaths. Domain II (25.0-28.5 °N, 119.3-123.5 °E, 41×10^3 km^2) has a strong seasonal variation in pCO_2. Domain III (28.5-33.0 °N, 126.0-128.0 °E, 96×10^3 km^2) is the northern ECS shelf generally dominated by temperature and impacted by the Changjiang plume in flood seasons. Domain IV (27.0-28.5 °N, 123.5-128.0 °E, 65×10^3 km^2) is the middle ECS shelf characterized by low Chl-*a* all year round and high pCO_2 in warm seasons. Domain V (25.0-27.0 °N, 120.0-125.4 °E, 60×10^3 km^2) is the southern ECS shelf where pCO_2 is dominated by temperature and might be under the influence of the northern Taiwan upwelling.

3 Material and Methods

3.1 Measurements of pCO_2, SST, SSS and auxiliary data

24 cruises/legs were conducted from 2006 to 2011 in the ECS on board R/Vs *Dongfanghong II* and *Kexue III* or a fishing boat Hubaoyu 2362. Survey periods and areas are listed in Table 2. Sampling tracks are shown in Fig. 2. During the cruises, sea surface salinity (SSS), SST and pCO_2 were measured continuously. The methods of measurement and data processing followed those of Pierrot et al. (2009) and the SOCAT (Surface Ocean CO_2 Atlas, http://www.socat.info/news.html) protocol, which are briefly summarized here.

pCO_2 was continuously measured with a non-dispersive infrared spectrometer (Li-Cor® 7000) integrated in a GO-8050 underway system (General Oceanic Inc. USA) on board Dongfanghong II or with a home-made underway system on board Kexue-III or Hubaoyu 2362. The GO-8050 underway system is described by Pierrot et al. (2009). The home-made underway system is described by Zhai et al. (2007) and Zhai and Dai (2009), with which a Jiang et al. (2008) equilibrator was employed. Surface water was continuously pumped from 1.5 to 5 m depth and determined every 80 seconds. CO_2 concentration in the atmosphere was determined every ~ 1.5 hours. The bow intake from which the air in the atmosphere was taken was installed ~ 10 m

above the sea surface to avoid contamination from the ship. The barometric pressure was measured continuously aboard with a barometer attached to a level of ~ 10 m above the sea surface. The accuracy of the pCO_2 measurements was ~ 0.3% (Zhai and Dai, 2009).

3.2 Data processing

Water pCO_2 at the temperature in the equilibrator (pCO_2^{Eq}) was calculated from the CO_2 concentration in the equilibrator (xCO_2) and the pressure in the equilibrator (P_{Eq}) after correction for the vapor pressure (P_{H2O}) of water at 100% relative humidity (Weiss and Price, 1980):

$$pCO_2^{Eq} = (P_{Eq} - P_{H2O}) \times xCO_2 \quad (1)$$

pCO_2 in the air was calculated similarly using xCO_2 in the air and the barometric pressure using a formula similar to Formula (1). xCO_2 in the atmosphere over the Tae-ahn Peninsula (36.7376 ℃N, 126.1328 ℃E, Republic of Korea, http://www.esrl.noaa.gov/gmd/dv/site) was adopted in the atmospheric pCO_2 calculation after comparison with the field measured values during the surveys.

Water pCO_2^{Eq} obtained from Formula (1) was corrected to pCO_2 at *in situ* temperature (*in situ* pCO_2, or pCO_2 hereafter) using the empirical formula of Takahashi et al. (1993), where t is the temperature in the equilibrator.

$$In\ situ\ pCO_2 = pCO_2^{Eq} \times \exp((SST-t) \times 0.0423) \quad (2)$$

Net CO_2 flux (F_{CO2}) between the surface water and the atmosphere (or air-sea CO_2 flux) was calculated using the following formula:

$$F_{CO2} = k \times s \times \Delta pCO_2 \quad (3)$$

where s is the solubility of CO_2 (Weiss, 1974); ΔpCO_2 is the pCO_2 difference between the surface water and the atmosphere; and k is the CO_2 transfer velocity. k was

parameterized using the empirical function of Sweeney et al. (2007) and nonlinear correction of gas transfer velocity with wind speed was adopted following Wanninkhof et al. (2002) and Jiang et al. (2008):

$$k(S07) = 0.27 \times C_2 \times U_{mean}^{2} \times (Sc/660)^{-0.5} \quad (4)$$

$$C_2 = \left(\frac{1}{n}\sum_{j=1}^{n} U_j^2\right)/U_{mean}^2 \quad (5)$$

where U_{mean} is the monthly mean wind speed at 10 m above the sea level (in m s^{-1}); and Sc is the Schmidt number at *in situ* temperature for surface seawater (Wanninkhof, 1992). C_2 is the nonlinear coefficient for the quadratic term of the gas transfer relationship; U_j is the high-frequency wind speed (in m s^{-1}); the subscript "mean" is to calculate the average; and n is the number of available wind speeds in the month. Wind speeds at a spatial resolution of 1°×1° and temporal resolution of 6 h were obtained from the National Centers for Environmental Prediction of the United States (NCEP, http://oceandata.sci.gsfc.nasa.gov/Ancillary/Meterological) and the monthly average was adopted in the CO_2 flux calculations. As defined here, a positive flux indicates an evasion of CO_2 from the sea to the air.

The seasonal amplitude and spatial variation in SST in the ECS are large, up to >10 ℃, which significantly impacts the pCO_2. To distinguish the influence of biogeochemical processes from the thermodynamics effect, pCO_2 was normalized to a constant temperature following Takahashi et al. (2002), termed as $NpCO_2$:

$$NpCO_2 = pCO_2 \times \exp(0.0423 \times (21 - SST)) \quad (6)$$

Here, 21 ℃ was used since it corresponded to the average SST during the cruises.

Our surveys covered the four seasons of the year, among which we defined March to May as spring, June to August as summer, September to November as fall and

December to February as winter.

At the global scale, both the atmospheric pCO_2 and the surface seawater pCO_2 are increasing and the rate of increase differs in different regions (Takahashi et al., 2009). Tseng et al. (2014) report that the increasing rate of pCO_2 is 1.9 and 2.1 μatm yr^{-1} for the atmosphere and the surface seawater, respectively, in the ECS based on the observations from 1998 to 2012. We assumed that these yearly change rates were evenly distributed to each month, based on which we corrected the pCO_2 data to June 2010.

4 Results

4.1 SST and SSS

Fig. 3 reveals strong temporal and spatial variations in SST over the 12 months of the year. The seasonal variation in the average SST and SSS in the five domains is further shown in Fig. 4 and Tables 3 to 7. In winter and spring, SST increased offshore and from north to south with a range of ~ 8 to 25 ℃, and the highest SST appeared in the southeastern part of the ECS. In summer and fall, SST was high and relatively spatially homogeneous compared to that in winter and spring with a range of ~18 to 30 ℃. On a monthly time scale, the lowest SST appeared in January to March and the highest in July to September (Fig. 3). The magnitude of seasonal variation in SST decreased offshore, from 12 to 14 ℃ in Domains I and II to 6 to 8 ℃ in Domains IV and V. The lowest SST was observed in Domain I in January 2009, which was 8.1±0.8 ℃ (Fig. 4). In July and August, there was a northeastern oriented filament with relatively low SST off eastern Taiwan (Fig. 3). The average SST measured underway during the surveys in the entire study area was 17.8±2.2 ℃ in winter, 19.7±2.9 ℃ in spring, 26.2±1.8 ℃ in summer and 23.2±1.2 ℃ in fall.

Spatially, salinity increased offshore and the highest salinity appeared in the area affected by the Kuroshio (not shown). At the whole shelf scale, the lowest salinity was observed in Domain I, where it was lower in March to August (29 to 32) and higher in

September to February (30 to 34). The low SSS in spring and summer corresponded to the high freshwater discharge of the year from the Changjiang. SSS in June was relatively high compared to that in March, April, May, July and August (Fig. 4B), which might be attributed to the fact that there was only one June survey (June 2011) and this survey followed an exceptionally dry May. The discharge of the Changjiang in May of 2011 was ~ 40% lower than the monthly average of 2005 to 2011 (data at Datong gauge station, the *Hydrological Information Annual Report* 2005 to 2011, Ministry of Water Resources, P. R. China). On a seasonal scale, the average SSS in Domain I was lowest in spring (30.6±4.6) and summer (30.9±1.4) and highest in fall (33.4±0.9). SSS in winter (31.5±2.3) was higher than in spring-summer but lower than in fall. The seasonality of SSS in Domain II was different from that of Domain I (Table 3), and was lower in November to February (29.6 to 34.3) than in March to October (32.6 to 34.0, Fig. 4B). This seasonality might be attributed to the fact that the Changjiang plume and coastal current were southwestward in winter (Han et al., 2013; Lee and Chao, 2003). The seasonal variation of SSS in Domains I and II was up to 2.7 to 2.8.

Data in Domain III were rather limited, based on which, SSS in winter (34.4±0.2) and fall (34.2±0.1) was higher than that in summer (33.1±0.6) (Table 5). The seasonality of SSS in Domains IV and V was similar, showing low SSS in July to September (33 to 34) but high in other months (>34). Seasonal variation in SSS in these two domains was <1, which was much smaller than that in Domains I, II and III. The average salinity in the entire study area was 33.2±2.5 in winter, 33.3±4.7 in spring, 33.0±1.6 in summer and 33.8±1.3 in fall.

4.2 Wind speeds and C_2

The temporal patterns of the wind speeds in the five domains were similar (Tables 3 to 7). The monthly average wind speeds ranged from 5.3 to 11.4 m s^{-1} and their standard deviations (SDs) were lower than 1 m s^{-1}. Generally, wind speed was high in fall and winter but low in spring and summer with great inter-annual variations. The

highest wind speeds were recorded in Domains II, IV and V in November 2007, when the monthly average wind speeds reached 10.4 to 11.4 m s^{-1}. The lowest wind speeds were observed in August 2008, May 2009 and May 2011, when the monthly average wind speeds ranged from 5.6 to 6.5 m s^{-1}. Wind speeds in September, October and November 2006 were relatively low compared to other fall months and, in March 2009, were relatively high compared to other spring months.

C_2 ranged from 1.06 to 1.70 and the annual average C_2 in the five domains was 1.21±0.04, 1.20±0.09, 1.21±0.06, 1.19±0.08 and 1.19±0.13, which was similar to or slightly lower than the global average of 1.27 (Wanninkhof et al., 2009).

4.3 CO_2 concentration in the air

Field observed CO_2 concentrations in the air over the ECS ranged 370 to 410 μatm, which was not inconsistent with the global increase in atmospheric pCO_2. Both the seasonal and inter annual patterns we measured during the surveys were similar to those observed at the Tae-ahn Peninsula (Korea-China Center for Atmospheric Research, Republic of Korea) with the highest values typically observed in February to April and the lowest values in July to September (Fig. 5). The difference in atmospheric CO_2 between our ship-board measurements over the ECS and that observed at the Tae-ahn Peninsula was not significant, ranging from 0.1 to 7.9 ppm (average ~ 3.5 ppm). However, the amplitude of the seasonal variation in air CO_2 concentration over the ECS was larger than that over the open North Pacific (Mauna Loa station), which was 5 to 10 ppm. Both the air CO_2 concentration over the ECS and the Tae-ahn Peninsula were higher than that at the Mauna Loa station, which might be due to the fact that the marine boundary atmosphere over marginal seas has more impacts from terrestrial sources.

4.4 Surface seawater pCO_2

pCO_2 values along the cruise tracks in this study are shown in Fig. 2. By averaging the pCO_2 values on these tracks to 1°×1° grids, we obtained the mean pCO_2 values in

the five domains (Tables 3 to 7).

For the entire ECS shelf, pCO_2 was relatively homogeneous in winter but strong spatial variations occurred in other seasons (Fig. 2). In Domain I, pCO_2 was generally low (<360 μatm) in winter, spring and summer except in the area off the Changjiang estuary mouth and in Hangzhou Bay and the northwestern corner which may be influenced by the southern Yellow Sea through the Yellow Sea Coastal Current (Su, 1998) that carried higher CO_2 water southward. However, in fall, pCO_2 was generally high (>380 μatm) except in October 2006. In Domain II, both the seasonal evolution and the pCO_2 values were generally overall similar to those of Domain I, but pCO_2 in summer was higher than in Domain I based on the limited data (Fig. 2). In Domains I and II, the seasonal average pCO_2 values were 348 and 349 μatm in winter, 309 and 313 μatm in spring, 317 and 357 μatm in summer, and 393 and 388 μatm in fall (Tables 3 and 4). The seasonal pattern in Domains IV and V was different showing relatively low pCO_2 (<360 μatm) in winter, spring and fall but high (>370 μatm) in summer (Fig. 2). The seasonal average pCO_2 values in these two domains were 341 and 344 μatm in winter, 318 and 345 μatm in spring, 380 and 381 μatm in summer and 336 and 348 μatm in fall (Tables 6 and 7). Temporal coverage was sparse in Domain III. Based on the limited data, the seasonality of pCO_2 in Domain III was similar to those of Domains IV and V (Table 5). The seasonal variation was largest in Domains I, II and III (~ 80 to 90 μatm) and smallest in Domain V (37 μatm).

In addition to the strong seasonal variation, intra-seasonal variation was also remarkable. In Domain I, the intra-seasonal variation in pCO_2 was ~ 30 to 73 μatm during the winter, spring and summer cruises, but relatively smaller in fall (<10 μatm excluding the October 2006 and December 2010 surveys, Table 3). In Domain II, it was much smaller in winter (<10 μatm) than in other seasons (30 to 80 μatm, Table 4). In Domains IV and V, it was ~ 10 μatm in winter, but relatively higher variability occurred in spring and summer (14 to 55 μatm, Tables 6 and 7).

Based on the seasonal average as shown in Fig. 6, the overall characteristics were

remarkable. In winter, the pCO_2 was relatively homogeneous and the average pCO_2 in each domain ranged from 340 to 349 μatm. In spring, the gridded pCO_2 values were lower than those in winter except in the northwest corner and the area near the Changjiang estuary. The seasonal average pCO_2 values in the domains were generally lower than in winter (309±60, 313±24, 290±10, 318±17 and 345±12 μatm in the five domains respectively) since the high pCO_2 values were located in very limited grids,. In summer, pCO_2 was lower in the inner shelf and higher in the outer shelf with extremely high pCO_2 in the northwest corner and off the Changjiang estuary mouth and Hangzhou Bay. The seasonal average pCO_2 was 317±72, 357±22, 341±18, 380±9.0 and 381±16 μatm in the five domains. In fall, the average pCO_2 was 393±40 μatm in Domain I, which was significantly higher than in the offshore domains (336 to 367 μatm).

It is worth noting that the two cruises conducted in October 2006 and December 2010 appeared to be atypical. The results in these two cruises were significantly different from other surveys in the respective seasons. In the October 2006 cruise, the pCO_2 went down to 364 μatm in Domain I and 308 μatm in Domain II, which was 29 and 80 μatm lower than the averages of other fall cruises in the two domains. In the December 2010 cruise, pCO_2 in Domain I was up to 384 μatm, which was 36 μatm higher than the average pCO_2 of the other winter cruises (Fig. 6). We will further discuss these cruises in the *Discussion* section.

The distribution of the SD of pCO_2 showed strong spatial and seasonal variations with a large range of 1 to 185 μatm (Fig. 6). In Domain I, the SD was low in winter and high in spring and summer. The highest SD occurred in summer in the coastal area off the Changjiang estuary mouth and in Hangzhou Bay with the highest value of 80 to 185 μatm. The SD in Domain II ranged from 1 to 48 μatm with higher values in spring and summer. In Domain III, the range of SD was 1 to 19 μatm and showed no remarkable seasonal pattern. In Domains IV and V, the SD range was 1 to 29 μatm with relatively higher values in spring and fall but lower in winter and summer in

Domain IV, and higher in spring and summer but lower in fall and winter in Domain V. Since pCO_2 distribution was generally homogeneous in winter except in December 2010, as expected, the SD in winter was relatively low and in >85% grids was <10 μatm and the highest SD was 17 μatm. The SD in October 2006 in Domain I was higher than the other fall surveys and the SD in Domain I in December 2010 was higher than the other winter surveys.

It should be noted that the SD of pCO_2 represents the mixture of sources of uncertainty in the gridded pCO_2 data, the analytical error, the spatial variance, and the bias from undersampling. Wang et al. (2014) demonstrate that the analytical errors are almost the same on the ECS shelf and the latitudinal distribution of SD is similar to that of the spatial variance. Thus, higher SD usually reflects higher spatial variance and vice versa along latitudes. However, the SD was equivalent to neither the spatial variance nor the bulk uncertainty and the bias from undersampling may exert the greatest uncertainty on the gridded pCO_2 in grids with poor sampling coverage (Wang et al., 2014).

4.5 Air-sea CO_2 fluxes

Similar to the different seasonality of pCO_2 in the differing domains, the air-sea CO_2 fluxes also had strong seasonal variations in each domain and the seasonal pattern differed among the domains (Tables 3 to 7).

Domain I was a sink of atmospheric CO_2 during all the winter, spring and summer surveys with CO_2 fluxes ranging from -14.0 to -1.6 mmol m^{-2} d^{-1}. However, Domain I in fall was a weak source of 2.2±6.8 mmol m^{-2} d^{-1}, with a flux range of 1.9 to 2.7 mmol m^{-2} d^{-1} (Table 3). The CO_2 fluxes we estimated were similar to those estimated by Zhai and Dai (2009) based on multiple observations (-10.4±2.3, -8.8±5.8, -4.9±4.0 and 2.9±2.9 mmol m^{-2} d^{-1} in winter, spring, summer and fall, respectively).

Similar to Domain I, Domain II was also a strong sink in winter and spring with a CO_2 flux range of -15.7 to -7.5 mmol m^{-2} d^{-1}. The seasonal average flux was -8.9±1.4

mmol m^{-2} d^{-1} in winter and -10.7±3.5 mmol m^{-2} d^{-1} in spring. The sink weakened in summer and the seasonal average CO_2 flux was -2.4±3.3 mmol m^{-2} d^{-1}. In fall, Domain II was a CO_2 source of 0.7±4.1 mmol m^{-2} d^{-1} (Table 4).

Although considerable variability occurred, Domains III, IV and V were generally strong sinks in winter, spring and fall (-3.7 to -18.7 mmol m^{-2} d^{-1}) but weak to moderate sources in summer (0 to 6.8 mmol m^{-2} d^{-1} except in June 2011 when it was a strong sink). On a seasonal time scale, CO_2 fluxes in Domains III, IV and V ranged from -10.0 to -10.8 mmol m^{-2} d^{-1} in winter, -6.8 to -17.8 mmol m^{-2} d^{-1} in spring; -3.7 to -9.3 mmol m^{-2} d^{-1} in fall; and 1.0 to 1.8 mmol m^{-2} d^{-1} in summer (Tables 5, 6 and 7).

The annual mean CO_2 fluxes were -6.2±9.1 mmol m^{-2} d^{-1} in Domain I, -5.3±3.7 mmol m^{-2} d^{-1} in Domain II, -9.2±4.2 mmol m^{-2} d^{-1} in Domain III, -7.5±1.7 mmol m^{-2} d^{-1} in Domain IV and -5.9±3.4 mmol m^{-2} d^{-1} in Domain V (Fig. 7). The area-weighted annual mean CO_2 flux was -6.9±(4.0) mmol m^{-2} d^{-1} (Fig. 7), which was more than twice the global average of ocean margins (Chen et al., 2013; Dai et al., 2013). Based on these CO_2 fluxes, the five domains absorbed 4.9(±4.4), 0.9(±0.4), 3.8(±1.0), 2.1(±0.3) and 1.5(±0.5)×10^{12} g C yr^{-1}, and the ECS shelf 13.2(±4.6)×10^{12} g C yr^{-1} of atmospheric CO_2.

5 Discussion

5.1 Major controls of surface water pCO_2

Because of the significant zonal difference in seasonality shown in both pCO_2 and CO_2 fluxes, we discuss the major controls of pCO_2 in the five domains categorized. This discussion is primarily based on the relationships of the *in situ* and normalized pCO_2 (NpCO_2, normalized to 21 ℃ in this study) with the other parameters in each domain. Since the Changjiang plume and coastal regions are strongly influenced by biological activities and/or the terrestrial high-pCO_2 waters (Tseng et al., 2014; Zhai and Dai, 2009), we used the data collected from the offshore area (Domains IV and V)

to obtain the "background" NpCO_2. In these two domains, NpCO_2 ranged from 250 to 400 μatm, and so we used 250×exp((SST-21)×0.0423) and 400×exp((SST-21)×0.0423) μatm as the lower and upper limits of thermodynamically dominated pCO_2 on the entire ECS shelf.

In Domains I and II, pCO_2 showed no conspicuous trend with SST on the yearly time scale (Fig. 8). However, within individual seasons, the temperature effect on pCO_2 can be generically revealed. In winter, most data were above the upper limit of the thermodynamically dominated pCO_2, suggesting extra CO_2 added to the surface water. In summer, many data were below the lower limit of the thermodynamically dominated pCO_2, indicating biogeochemical uptake of CO_2. The pCO_2 in these two domains neither showed clear trends with salinity but in winter, it generally decreased with SSS (Fig. 9). It is thus suggested that other processes in addition to SST and estuarine mixing also played important roles in the pCO_2 variability, including aerobic respiration, biological productivity, terrestrial input and ventilation, amongst other factors.

The Changjiang river and estuarine water were characterized by high pCO_2 resulting mainly from aerobic respiration (Zhai et al., 2007). In Domain I, the area off the Changjiang estuary and the coastal area were influenced by the high-pCO_2 estuarine water (Fig. 2). On the other hand, in warm seasons, the plume water was stratified and biological productivity lowered the surface water pCO_2 as indicated by the high Chl-*a* concentration in spring and summer (Fig. 10). NpCO_2 generally decreased with the increase in Chl-*a* concentration. Although pCO_2 showed no relationship with SST or SSS, NpCO_2 showed a decreasing pattern with SST and the lowest NpCO_2 occurred in the warm seasons, which was consistent with the highest productivity (Figs 8 and 10). In fall, vertical stratification collapsed and the CO_2-enriched subsurface and bottom waters mixed into the surface and increased the surface water pCO_2. In winter and early fall, the cooling effect decreased pCO_2 and resulted in Domain I acting as a CO_2 sink in the cold seasons. If the pCO_2 in winter was taken as the reference, the

calculated thermodynamically controlled pCO_2 in spring would be 379.3 μatm. The observed pCO_2 in spring was 70.4 μatm lower than the thermodynamically mediated pCO_2. Similarly, if spring was taken as a reference, the thermodynamically mediated pCO_2 in summer would be 479.0 μatm and the observed pCO_2 was 161.8 μatm lower than this value. These differences might be the CO_2 drop mainly mediated by biological activities. Similarly, the observed pCO_2 was 100.5 μatm higher than the thermodynamically mediated pCO_2 (293.0 μatm) in fall, which might be due mainly to the mixing of the CO_2-rich subsurface/bottom water in fall, when vertical mixing was enhanced. It should be noted that the CO_2 system is a buffer system and the pCO_2 response is much slower (Zhai et al., 2014). Therefore the above estimation is to explain the biological effect on pCO_2 qualitatively rather than to make an accurate calculation.

Controls of pCO_2 in Domain II were similar to but more complex than those in Domain I. Cooling and biological uptake were responsible for the strong sink in winter and spring. However, in summer biological uptake of CO_2 was limited since it was beyond the productive area (Fig. 10), so the CO_2 flux was controlled by both biological activities and heating effect. In fall, cooling was important in drawing down pCO_2 and the influence of vertical mixing was not significant since the hypoxia and thus the high-pCO_2 bottom water was limited to Domain I (Chen et al., 2007; Wang et al., 2012).

In Domains IV and V, pCO_2 in summer was higher than that in the other seasons (Fig. 2). The pCO_2 generally increased with SST but showed no trend with SSS (Figs 8 and 9). This suggests that temperature was an important factor influencing pCO_2. Neither pCO_2 nor NpCO_2 showed conspicuous trends with Chl-*a* concentration, and Chl-*a* concentration was relatively low (<2 μg L^{-1}, Fig. 10). This suggests that, for a particular season, productivity was not the dominating process in the spatial distribution of pCO_2. Comparison among the seasons showed that the NpCO_2 was highest in winter and lowest in summer. This might be due to the weak mixing of the

CO_2-rich subsurface water in summer. Additionally, the lowest NpCO_2 values in summer might suggest that the potential biological uptake of CO_2 was strong in summer, although biological uptake was not a dominating factor. Although NpCO_2 was lowest in summer, *in situ* pCO_2 was highest, indicating that high temperature increased pCO_2 in the warm seasons. With similar calculations conducted in Domain I, the estimated pCO_2 drawdown would be 25 to 39 μatm in spring and summer and the pCO_2 increase in fall would range from 21 to 35 μatm due to enhanced vertical mixing. These values were much lower than the dynamic inshore areas (Domains I and II) and might be negligible since the above estimations were very rough and the re-equilibrium of CO_2 takes a longer time than any particular season (Zhai et al., 2014). The major controls of pCO_2 in Domain III were between those of Domains I/II and IV/V.

In summary, the ECS shelf is heterogeneous in both CO_2 fluxes and their controls. The pCO_2 of the inner shelf waters (Domains I and II) was mainly dominated by the biological uptake of CO_2 in spring/summer and cooling in winter, which induced the moderate to strong sink in the three seasons, while in fall mixing with CO_2-rich bottom/subsurface water was attributed to the CO_2 release. However, the offshore areas (Domains IV and V) were dominated mainly by temperature.

The CO_2 sink is dominated by the high biological productivity in summer (Chou et al., 2009), which appears to have close correlation with the Changjiang riverine discharge (Tseng et al., 2011; Tseng et al., 2014). However, cooling is attributed to be the major driver of the CO_2 sink in winter (Tsunogai et al., 1999). In the northern ECS and in the area off the Changjiang estuary, vertical mixing of the CO_2-rich subsurface/bottom waters is attributed to the CO_2 source in fall (Kim et al., 2013; Zhai and Dai, 2009). Shim et al. (2007) suggest that pCO_2 in the northeastern ECS is dominated by temperature but in the northwestern ECS, the main controlling factor is more seasonally complex. Based on the data collected from single cruise in summer, fall and winter, Chou et al. (2013) suggest that pCO_2 is dominated by biological

production on the inner shelf and by temperature on the outer shelf.

Based on the data collected mainly in the inner and middle ECS shelves and limited field surveys in cold seasons, Tseng et al. (2014) suggest that the Changjiang discharge is the primary factor that governs the CO_2 sink for the entire ECS. The dataset covering complete seasonal and spatial coverage presented in this study suggested that zonal assessment is important to obtain a comprehensive picture of CO_2 flux and its control in the dynamic marginal seas. Extrapolation from the data collected in the river-dominated area to the entire ECS shelf could be misleading.

5.2 Intra-seasonal variation in CO_2 fluxes

With the five domains categorized, we have seen overall well defined seasonality in both pCO_2 and CO_2 fluxes in the individual domains, and significant intra-seasonal changes occurred, which could affect the overall carbon budgeting on a longer seasonal and/or annual time scale.

The intra-seasonal variation in the CO_2 fluxes was generally low in winter (typically <2 fold variations), but it was very high in summer (4 to 6 fold) and spring (2 to 3 fold). Spatially, the largest intra-seasonal variability was in Domain I. The intra-seasonal variation in the calculated CO_2 flux in this study was attributed to the intra-seasonal variability in ΔpCO_2, wind speeds, and C_2. In the five domains, the highest value of C_2 was 1.1 to 1.4 fold of the lowest value within each season, which did not induce remarkable intra-seasonal variability in the calculated CO_2 flux. However, intra-seasonal variability in wind speed and ΔpCO_2 might have induced large variability in the calculated CO_2 fluxes. The highest wind speed was 1.1 to 1.2 fold the lowest value in winter and 1.2 to 1.6 fold those in spring, summer and fall in each domain. This might have caused 1.2 to 1.4 fold variation in winter and 1.4 to 2.6 fold variation in other seasons in the calculated CO_2 fluxes. The intra-seasonal variability in wind speed showed no spatial pattern. The intra-seasonal variation in ΔpCO_2 was generally high in summer and spring but low in winter and fall. The

largest intra-seasonal variation was observed in Domain I in summer and spring. In summer, the lowest ΔpCO_2 was -85 μatm in June 2006, which was 6.9 fold that in July 2009 (-12 μatm). The intra-seasonal variation in ΔpCO_2 in spring was smaller than in summer but still very large (3.5 fold).

Additionally, atypical surveys increased the intra-seasonal variations. One example was the October 2006 cruise. Under typical fall conditions, Domain I is a source of atmospheric CO_2 when stratification starts to weaken and strong vertical mixing starts leading to the release of subsurface CO_2 (Zhai and Dai, 2009). In October 2006, however, average pCO_2 was down to 364 μatm in Domain I, which was 29 μatm lower than the seasonal average based on the data collected during all the other surveys in fall (394 μatm) (Table 3). The low pCO_2 in Oct 2006 might be induced by a local bloom which was reflected by the high oxygen saturation degree in the surface water. Dissolved oxygen increased to 120% to 130% in a local area off Hangzhou Bay and the Changjiang estuary, which was a significant increase from September 2006 when the oxygen saturation degree ranged from 90 to 110% (Fig. A1 in the Appendix). This local bloom caused Domain I to act as a CO_2 sink of 1.9 mmol m^{-2} d^{-1} as compared to a CO_2 source of 2.2 mmol m^{-2} d^{-1} based on the data collected from all the other fall surveys (Table 3). If this survey was included into the flux estimation, the seasonal average CO_2 flux in fall would be 1.2±6.4 in Domain I. This CO_2 source strength was ~ 54% of the average of the other fall cruises in Domain I. However, inclusion of the October 2006 survey into the fall cruises would result in an annual CO_2 flux of -7.1± 3.9 mmol m^{-2} d^{-1}, which is not significantly different from the estimate of -6.9±4.0 mmol m^{-2} d^{-1} excluding the October 2006 cruise. This was because we had multiple cruise observations in fall and the fall bloom was only observed in a very small area of the ECS. b

In the temperate seas, blooms occur in both spring and fall, which are mainly controlled by light availability and nutrient supply (Lalli and Parsons, 1993; Martinez et al., 2011). In the ECS, there is no report on fall blooms in the near shore area. The

occurrence of a fall bloom and its influence on the CO_2 flux needs further study.

Another example is the early winter cruise (based on our seasonal category) in 2010 which was conducted on 1-11 December. The average SST was 5.5 ℃ higher than the average SST during other winter surveys in Domain I. Also, the pCO_2 distribution pattern was similar to that in fall. As a result, Domain I was a weak sink of -1.6 mmol m^{-2} d^{-1} during this early December cruise, which was only 16% of the average CO_2 sink based on the data collected during the other winter cruises (-9.8 mmol m^{-2} d^{-1}). We concluded that this early December 2010 survey was conducted during the transitional period between typical fall and winter, which would be difficult to be categorized into any season. If the December 2010 survey was grouped into the fall cruises, the seasonal average CO_2 flux in Domain I in fall would be 1.2±7.1 mmol m^{-2} d^{-1} and the annual CO_2 flux in the entire ECS would be -7.4±4.1 mmol m^{-2} d^{-1}. However, if the December 2010 survey was grouped into the winter cruises, the seasonal average CO_2 flux in Domain I in winter would be -8.4±5.3 mmol m^{-2} d^{-1} and the annual CO_2 flux in the entire ECS would be -6.9±4.1 mmol m^{-2} d^{-1}.

The strong CO_2 sink in the ECS might be attributed to the generally low surface water pCO_2. As discussed in Section 5.1, the strong biological uptake in spring/summer and strong cooling in winter were the major controls of the low pCO_2 in the ECS. Primary production on the ECS shelf ranges from 0.2 to 2.0 g C m^{-2} d^{-1} in warm seasons (Gong et al., 2003). During our spring and summer cruises, Chl-*a* concentration was up to 20 or even 40 μg L^{-1}. Both the phytoplankton biomass and the primary production are among the highest in the world marginal seas such as the Barents Sea (Dalpadado et al., 2014) , the Beaufort Sea (Carmack et al., 2004), the South Atlantic Bight (Martins and Pelegri, 2006), and the South China Sea (Chen, 2005). In addition, the ECS is located in the mid latitude zone with strong seasonality. In winter, the low temperature draws surface water pCO_2 well below the atmospheric pCO_2, drawing down ~ 140 μatm with 10 ^{o}C decrease from ~ 400 μatm.

This study reports what we believe to be a most comprehensive dataset of CO_2 fluxes

based on field measurements with a full coverage of the ECS shelf at a temporal resolution of seasonal scale. Table 8 shows comparisons of the CO_2 fluxes estimated in this study with others in the ECS. For ease of comparison, we standardized the CO_2 flux estimation using the Sweeney et al. (2007) gas transfer velocity algorithms. For the results calculated using long-term (or monthly) average wind speeds, we multiplied C_2 (~ 1.2) to make them consistent with our estimation. The CO_2 fluxes calculated using the algorithm of Ho et al. (2006) were the same as those of Sweeney et al. (2007).

Comparison between our results and the CO_2 fluxes estimated based on multiple observations (such as those of Zhai and Dai 2009) were similar in Domain I in all seasons (the differences were <35%, Table 8). However, the CO_2 flux estimations based on limited surveys in spring, the season with strong intra-seasonal variability, such as those of Kim et al. (2013) and Shim et al. (2007) in Domains I and III, and Peng et al. (1999) in Domains III, IV and V, were often different from our results. However, the CO_2 flux based on a single survey in winter by Chou et al. (2011) on the entire ECS shelf, Shim et al. (2007) and Kim et al. (2013) in Domains I and III were similar to our results, which is likely due to the relatively smaller inter-seasonal variability in winter. For the entire ECS, The CO_2 fluxes in spring and summer estimated by Tseng et al. (2011; 2014) are similar to our estimate based on field surveys. However, there is a large difference in the fall results. The good consistency of the Tseng et al. (2011; 2014) results with ours in spring and summer might be due to the fact that their empirical algorithm is mainly based on field data collected in warmer seasons.

We have demonstrated that field observations with full consideration of seasonal variability is necessary to constrain CO_2 fluxes with large heterogeneity in both time and space. We must point out, however, that it remains difficult to fully resolve the intra-seasonal changes in dynamic shelf seas, in particularly in areas such as Domains I and II. High-frequency observation in the seasons and/or locations with largest

variability and/or with poor understanding in the mechanisms controlling pCO_2 are clearly needed to reduce the error from undersampling are mandatory to further improve estimates of CO_2 fluxes.

6 Concluding remarks

Surface water pCO_2 and air-sea CO_2 fluxes in the ECS shelf show strong temporal and spatial variations, despite which, the pCO_2 and associated fluxes are robustly well defined. The Changjiang plume is a moderate to strong CO_2 sink in spring, summer and winter, but it is a weak CO_2 source in fall. The middle and southern ECS shelves are a CO_2 source in summer but a strong CO_2 sink in other seasons. Major controls of pCO_2 differ in different domains. Domains I and II were mainly dominated by biological CO_2 uptake in spring and summer, ventilation in fall and cooling in winter, while Domains IV and V were dominated by temperature over the whole year. On an annual basis, the entire ECS shelf is a CO_2 sink of 6.9 (±4.0) mmol m^{-2} d^{-1} and it sequesters 13.2 Tg C from the atmosphere annually based on our observations from 2006 to 2011. This study suggested that zonal assessment of CO_2 fluxes and study of the major controls is necessary in the dynamic marginal seas.

Acknowledgements

This study was jointly supported by the National Basic Research Program of China through grant 2009CB421200 (the CHOICE-C project) and 2015CB954001 (CHOICE-C II), and Natural Science Foundation of China through grants 41076044 and 41121091, and the State Oceanic Administration of China through contract DOMEP-MEA-01-10. Sampling cruises were partially supported by the National High-Tech Research and Development Program ("863" Program) of China (via the projects of Quality Control / *in situ* Standardization Experiment 2007 and 2008) and the National Basic Research Program of China (grant 2005CB422300). We are grateful to the crew and scientific staff of R/V Dongfanghong II for their help during these large-scale surveys. Yuancheng Su and Jinwen Liu are appreciated for the data collection during some of the cruises. We acknowledge the constructive comments

from three anonymous reviewers, which improved the quality of our paper. Professor John Hodgkiss of The University of Hong Kong is thanked for polishing the English in this paper.

References

Bai, Y., He, X., Pan, D., Chen, C.-T.A., Kang, Y., Chen, X. and Cai, W.-J., 2014. Summertime Changjiang River plume variation during 1998–2010. Journal of Geophysical Research: Oceans, 119(9): 6238-6257.

Borges, A.V., Delille, B. and Frankignoulle, M., 2005. Budgeting sinks and sources of CO_2 in the coastal ocean: Diversity of ecosystems counts. Geophysical Research Letters, 32(14): L14601, doi:10.1029/2005GL023053.

Cai, W.-J., Dai, M.H. and Wang, Y.-C., 2006. Air-sea exchange of carbon dioxide in ocean margins: A province-based synthesis. Geophysical Research Letters, 33(12): L12603, doi:10.1029/2006GL026219.

Carmack, E.C., Macdonald, R.W. and Jasper, S., 2004. Phytoplankton productivity on the Canadian Shelf of the Beaufort Sea. Marine Ecology Progress Series, 277: 37-50.

Chen, C.C., Gong, G.C. and Shiah, F.K., 2007. Hypoxia in the East China Sea: One of the largest coastal low-oxygen areas in the world. Marine Environmental Research, 64(4): 399-408.

Chen, C.T.A. and Borges, A.V., 2009. Reconciling opposing views on carbon cycling in the coastal ocean: Continental shelves as sinks and near-shore ecosystems as sources of atmospheric CO_2. Deep-Sea Research II, 56(8-10): 578-590.

Chen, C.T.A., Huang, T.H., Chen, Y.C., Bai, Y., He, X. and Kang, Y., 2013. Air-sea exchanges of CO_2 in the world's coastal seas. Biogeosciences, 10(10): 6509-6544.

Chen, C.T.A. and Wang, S.L., 1999. Carbon, alkalinity and nutrient budgets on the East China Sea continental shelf. Journal of Geophysical Research, 104(C9): 20675-20686.

Chen, Y.-L.L., 2005. Spatial and seasonal variations of nitrate-based new production

and primary production in the South China Sea. Deep-Sea Research I, 52(2): 319-340.

Chou, W.-C., Gong, G.-C., Cai, W.-J. and Tseng, C.-M., 2013. Seasonality of CO_2 in coastal oceans altered by increasing anthropogenic nutrient delivery from large rivers: evidence from the Changjiang–East China Sea system. Biogeosciences, 10: 3889-3899.

Chou, W.C., Gong, G.C., Sheu, D.D., Hung, C.C. and Tseng, T.F., 2009. Surface distributions of carbon chemistry parameters in the East China Sea in summer 2007. Journal of Geophysical Research, 114(C07): C07026, doi:10.1029/2008JC005128.

Chou, W.C., Gong, G.C., Tseng, C.M., Sheu, D.D., Hung, C.C., Chang, L.P. and Wang, L.W., 2011. The carbonate system in the East China Sea in winter. Marine Chemistry, 123(1-4): 44-55.

Chou, W.C., Sheu, D.D., Lee, B.S., Tseng, C.M., Chen, C.T.A., Wang, S.L. and Wong, G.T.F., 2007. Depth distributions of alkalinity, TCO_2 and $\delta\ ^{13}C$ (TCO_2) at SEATS time-series site in the northern South China Sea. Deep-Sea Research II, 54(14-15): 1469-1485.

Dai, A. and Trenberth, K.E., 2002. Estimates of freshwater discharge from continents: Latitudinal and seasonal variations. Journal of Hydrometeorology, 3(6): 660-687.

Dai, M., Cao, Z., Guo, X., Zhai, W., Liu, Z., Yin, Z., Xu, Y., Gan, J., Hu, J. and Du, C., 2013. Why are some marginal seas sources of atmospheric CO_2? Geophysical Research Letters, 40: 2154-2158.

Dalpadado, P., Arrigo, K.R., Hjollo, S.S., Rey, F., Ingvaldsen, R.B., Sperfeld, E., van Dijken, G.L., Stige, L.C., Olsen, A. and Ottersen, G., 2014. Productivity in the Barents Sea - Response to Recent Climate Variability. Plos One, 9(5).

Gong, G.C., Wen, Y.H., Wang, B.W. and Liu, G.J., 2003. Seasonal variation of chlorophyll a concentration, primary production and environmental conditions in the subtropical East China Sea. Deep-Sea Research II, 50(6-7): 1219-1236.

Han, A., Dai, M., Gan, J., Kao, S., Zhao, X.Z., Jan, S., Li, Q., Lin, H., Chen, C.T.A.,

Wang, L., Hu, J., Wang, L. and Gong, F., 2013. Inter-shelf nutrient transport from the East China Sea as a major nutrient source supporting winter primary production on the northern South China Sea shelf. Biogeosciences, 10: 8159-8170.

He, X., Bai, Y., Pan, D., Chen, C.-T.A., Cheng, Q., Wang, D. and Gong, F., 2013. Satellite views of seasonal and inter-annual variability of phytoplankton blooms in the eastern China seas over the past 14 yr (1998-2011). Biogeosciences, 10(7): 4721-4739.

Ho, D.T., Law, C.S., Smith, M.J., Schlosser, P., Harvey, M. and Hill, P., 2006. Measurements of air-sea gas exchange at high wind speeds in the Southern Ocean: Implications for global parameterizations. Geophysical Research Letters, 33(16): L16611, doi:10.1029/2006GL026817.

Jiang, L.Q., Cai, W.J., Wanninkhof, R., Wang, Y.C. and Luger, H., 2008. Air-sea CO2 fluxes on the US South Atlantic Bight: Spatial and seasonal variability. Journal of Geophysical Research-Oceans, 113(C7): C07019, doi:10.1029/2007JC004366.

Kim, D., Choi, S.-H., Shim, J.-H., Kim, K.-H. and Kim, C.-H., 2013. Revisiting the seasonal variations of sea-air CO_2 fluxes in the northern East China Sea. Terrestrial Atmospheric and Oceanic Sciences, 24(3): 409-419.

Lalli, C.M. and Parsons, T.R., 1993. Biological Oceanography: An Introduction. Butterworth Heinemann, Burlington.

Laruelle, G.G., Durr, H.H., Slomp, C.P. and Borges, A.V., 2010. Evaluation of sinks and sources of CO_2 in the global coastal ocean using a spatially-explicit typology of estuaries and continental shelves. Geophysical Research Letters, 37(15): L15607, doi:10.1029/2010GL043691.

Laruelle, G.G., Lauerwald, R., Pfeil, B. and Regnier, P., 2014. Regionalized global budget of the CO_2 exchange at the air-water interface in continental shelf seas. Global Biogeochemical Cycles, 28(11): 1199-1214.

Lee, H.J. and Chao, S.Y., 2003. A climatological description of circulation in and around the East China Sea. Deep-Sea Research II, 50(6-7): 1065-1084.

Liss, P.S. and Merlivat, L., 1986. Air-sea gas exchange rates: introduction and synthesis. In: P. Buat-Menard (Editor), The Role of Air-Sea Exchange in Geochemical Cycling. Reidel, Hingham, MA, pp. 113-129.

Liu, Z. and Gan, J., 2012. Variability of the Kuroshio in the East China Sea derived from satellite altimetry data. Deep-Sea Research I, 59: 25-36.

Martinez, E., Antoine, D., D'Ortenzio, F. and de Boyer Montegut, C., 2011. Phytoplankton spring and fall blooms in the North Atlantic in the 1980s and 2000s. Journal of Geophysical Research, 116(C11): C11029, doi:10.1029/2010JC006836.

Martins, A.M. and Pelegri, J.L., 2006. CZCS chlorophyll patterns in the South Atlantic Bight during low vertical stratification conditions. Continental Shelf Research, 26(4): 429-457.

Omar, A., Johannessen, T., Kaltin, S. and Olsen, A., 2003. Anthropogenic increase of oceanic pCO_2 in the Barents Sea surface water. Journal of Geophysical Research, 108(C12): 3388, doi:10.1029/2002JC001628.

Peng, T.H., Hung, J.J., Wanninkhof, R. and Millero, F.J., 1999. Carbon budget in the East China Sea in spring. Tellus B, 51(2): 531-540.

Pierrot, D., Neill, C., Sullivan, K., Castle, R., Wanninkhof, R., Luger, H., Johannessen, T., Olsen, A., Feely, R.A. and Cosca, C.E., 2009. Recommendations for autonomous underway pCO_2 measuring systems and data-reduction routines. Deep-Sea Research II, 56(8-10): 512-522.

Shim, J., Kim, D., Kang, Y.C., Lee, J.H., Jang, S.T. and Kim, C.H., 2007. Seasonal variations in pCO_2 and its controlling factors in surface seawater of the northern East China Sea. Continental Shelf Research, 27(20): 2623-2636.

Su, J., 1998. Circulation dynamics of the China Seas north of 18 N coastal segment. In: A.R. Robinson and K.H. Brink (Editors), The Sea (Vol. 11). John Wiley & Sons, Inc., New York, pp. 483-505.

Sweeney, C., Gloor, E., Jacobson, A.R., Key, R.M., McKinley, G., Sarmiento, J.L. and Wanninkhof, R., 2007. Constraining global air-sea gas exchange for CO_2 with recent bomb C-14 measurements. Global Biogeochemical Cycles, 21(2):

GB2015, doi:10.1029/2006GB002784.

Takahashi, T., Olafsson, J., Goddard, J.G., Chipman, D.W. and Sutherland, S.C., 1993. Seasonal variation of CO_2 and nutrients in the high latitude surface oceans-A comparative study. Global Biogeochemical Cycles, 7(4): 843-878.

Takahashi, T., Sutherland, S.C., Sweeney, C., Poisson, A., Metzl, N., Tilbrook, B., Bates, N., Wanninkhof, R., Feely, R.A., Sabine, C., Olafsson, J. and Nojiri, Y., 2002. Global sea-air CO2 flux based on climatological surface ocean pCO_2, and seasonal biological and temperature effects. Deep-Sea Research II, 49(9-10): 1601-1622.

Takahashi, T., Sutherland, S.C., Wanninkhof, R., Sweeney, C., Feely, R.A., Chipman, D.W., Hales, B., Friederich, G., Chavez, F., Sabine, C., Watson, A., Bakker, D.C.E., Schuster, U., Metzl, N., Yoshikawa-Inoue, H., Ishii, M., Midorikawa, T., Nojiri, Y., Kortzinger, A., Steinhoff, T., Hoppema, M., Olafsson, J., Arnarson, T.S., Tilbrook, B., Johannessen, T., Olsen, A., Bellerby, R., Wong, C.S., Delille, B., Bates, N.R. and de Baar, H.J.W., 2009. Climatological mean and decadal change in surface ocean pCO_2, and net sea-air CO_2 flux over the global oceans. Deep-Sea Research II, 56(8-10): 554-577.

Tans, P.P., Fung, I.Y. and Takahashi, T., 1990. Observational constraints on the global atmospheric CO_2 budget. Science, 247(4949): 1431-1438.

Tseng, C.-M., Liu, K.K., Gong, G.C., Shen, P.Y. and Cai, W.J., 2011. CO_2 uptake in the East China Sea relying on Changjiang runoff is prone to change. Geophysical Research Letters, 38: L24609, doi:10.1029/2011GL049774.

Tseng, C.M., Shen, P.-Y. and Liu, K.-K., 2014. Synthesis of observed air-sea CO_2 exchange fluxes in the river-dominated East China Sea and improved estimates of annual and seasonal net mean fluxes. Biogeosciences, 11: 3855-3870.

Tsunogai, S., Watanabe, S. and Sato, T., 1999. Is there a "continental shelf pump" for the absorption of atmospheric CO_2? Tellus B, 51(3): 701-712.

Wang, B.D., Wei, Q.S., Chen, J.F. and Xie, L.P., 2012. Annual cycle of hypoxia off the Changjiang (Yangtze River) Estuary. Marine Environmental Research, 77:

1-5.

Wang, G., Dai, M., Shen, S.S., Bai, Y. and Xu, Y., 2014. Quantifying uncertainty sources in the gridded data of sea surface CO_2 patial pressure. Journal of Geophysical Research-Oceans, 119(8): 5181-5189.

Wang, S.L., Chen, C.T.A., Hong, G.H. and Chung, C.S., 2000. Carbon dioxide and related parameters in the East China Sea. Continental Shelf Research, 20(4-5): 525-544.

Wanninkhof, R., 1992. Relationship between wind speed and gas exchange over the ocean. Journal of Geophysical Research, 97(C05): 7373-7382.

Wanninkhof, R., Asher, W.E., Ho, D.T., Sweeney, C. and McGillis, W.R., 2009. Advances in quantifying air-sea gas exchange and environmental forcing. Annual Review of Marine Science, 1: 213-244.

Wanninkhof, R., Doney, S.C., Takahashi, T. and McGillis, W., 2002. The effect of using time-averaged winds on regional air-sea CO_2 fluxes. In: M.A. Donelan (Editor), Gas Transfer at Water Surfaces, Geophys. Monogr. Ser., Volume 127. Amrican Geophysical Union, Washington, D.C., doi:10.1029/GM127p0351, pp. 351-357.

Weiss, R.F., 1974. Carbon dioxide in water and seawater: the solubility of a non-ideal gas. Marine Chemistry, 2: 203-215.

Weiss, R.F. and Price, B.A., 1980. Nitrous oxide solubility in water and seawater. Marine Chemistry, 8(4): 347-359.

Zhai, W., Chen, J., Jin, H., Li, H., Liu, J., He, X. and Bai, Y., 2014. Spring carbonate chemistry dynamics of surface waters in the northern East China Sea: Water mixing, biological uptake of CO_2, and chemical buffering capacity. Journal of Geophysical Research, 119: 5638-5653.

Zhai, W.D. and Dai, M.H., 2009. On the seasonal variation of air-sea CO_2 fluxes in the outer Changjiang (Yangtze River) Estuary, East China Sea. Marine Chemistry, 117(1-4): 2-10.

Zhai, W.D., Dai, M.H. and Guo, X.H., 2007. Carbonate system and CO_2 degassing fluxes in the inner estuary of Changjiang (Yangtze) River, China. Marine

798 Chemistry, 107(3): 342-356.

799

800

801 Table 1 Summary of the five physico-biogeochemical domains categorized in the East China Sea.
802

Domain	Location	Longitude (°E)	Latitude (°N)	Surface area (10^4 km^2)	Description & Characteristics
I	Outer Changjiang Estuary and Changjiang plume	122-126	28.5-33	19.1	Lower estuary beyond the turbidity maximum zone and inner shelf influenced by river plume
II	Zhejiang-Fujian coast	119.33-123.5	25-28.5	4.1	Inner shelf dominated by turbid coastal waters with the influence of river plume primarily in winter.
III	Northern East China Sea	126-128	28.5-33	9.6	Mid- and outer shelf influenced by the Kuroshio. River plume signals visible in flood seasons.
IV	Middle East China Sea	122-128	27-28.5	6.5	Mid- and outer shelf influenced by the Kuroshio.
V	Southern East China Sea	120-125.42	25-27	6.0	Mid- and outer shelf influenced by the Kuroshio and characterized by upwelling northern Taiwan.

803
804

805 Table 2 Summary information of the 24 sampling surveys from 2006 to 2011.

Surveying time	Surveyed zones	Season	Sampling depth/RV	Sampler configuration	References/data source
1-3 January 2006	I	Winter	1.5 m (Fishing boat Hubaoyu 2362)	Modified from Zhai et al. (2007)	Zhai et al., 2007; Zhai and Dai, 2009
18-25 September 2006	I, II	Fall	3 m (Kexue 3)	Modified from Jiang et al. (2008)	This study [a]
14-17 October 2006	I, II, IV	Fall	3 m (Kexue 3)	Modified from Jiang et al. (2008)	This study [a]
20-24 November 2006	I, II	Fall	5 m (Dongfanghong 2)	Modified from Jiang et al. (2008)	This study [a]
2-6 July 2007	I, II, V	Summer	5 m (Dongfanghong 2)	Modified from Jiang et al. (2008)	This study [a]
1-10 November 2007	I, III	Fall	5 m (Dongfanghong 2)	GO8050	Zhai and Dai, 2009
20-30 April 2008	I, II	Spring	5 m (Dongfanghong 2)	GO8050	This study [a]
6-29 August 2008	I, II, IV, V	Summer	5 m (Dongfanghong 2)	GO8050	This study
23-31 December 2008	I, II. V	Winter	5 m (Dongfanghong 2)	GO8050	This study
10-14 January 2009	I, II	Winter	5 m (Dongfanghong 2)	GO8050	This study
15-31 March 2009	I, II, IV, V	Spring	5 m (Dongfanghong 2)	GO8050	This study
6-10 April 2009	I	Spring	1.5 m (Hubaoyu 2362)	Modified from Jiang et al. (2008)	This study
4-30 April 2009	I, II, III, IV, V	Spring	5 m (Dongfanghong 2)	GO8050	This study
1-13 May 2009	I, II, IV, V	Spring	5 m (Dongfanghong 2)	GO 8050	This study
1-3 July 2009	I, II, IV, V	Summer	5 m (Dongfanghong 2)	GO8050	Wang et al. (2014)
17-31 August 2009	I, II, III, IV, V	Summer	5 m (Dongfanghong 2)	GO8050	Wang et al. (2014)
4-31 December 2009	I, II, III, IV, V	Winter	5 m (Dongfanghong 2)	GO8050	This study
1-5 January 2010	II, IV, V	Winter	5 m (Dongfanghong 2)	GO8050	This study
1-6 February 2010	I, II	Winter	5 m (Dongfanghong 2)	GO8050	This study
26-30 November 2010	II, IV, V	Fall	5 m (Dongfanghong 2)	GO8050	This study
1-11 December 2010	I, III, IV	Winter	5 m (Dongfanghong 2)	GO8050	This study
13-15 April 2011	I, IV, V	Spring	5 m (Dongfanghong 2)	GO8050	This study
28-30 May 2011	II, III, IV, V	Spring	5 m (Dongfanghong 2)	GO8050	This study
1-8 June 2011	I, II, III, IV	Summer	5 m (Dongfanghong 2)	GO8050	This study

806 [a] Partially published in Zhai and Dai (2009).

807

808 Table 3 Data summary of Domain I. Atm. pCO_2 is atmospheric pCO_2; SST is sea surface temperature; SSS is sea surface salinity; F_{CO2} is the
809 air-sea CO_2 flux, and SD is standard deviation. C_2 is the nonlinearity effect of the short-term variability of wind speeds over a month on the gas
810 transfer velocity, assuming long-term winds followed a Raleigh (Weibull) distribution (Wanninkhof, 1992; Jiang et al., 2008). See text for details.
811 October 2006 and December 2010 were excluded in the calculations of seasonal averages. pCO_2 data are corrected to the reference year 2010.

Season	Period	pCO_2 (μatm)		Atm. pCO_2 (μatm)		ΔpCO_2 (μatm)		SST (℃)		SSS		Wind speed (m s^{-1})		C_2	FCO_2 (mmol m^{-2} d^{-1})	
		Mean	SD	Mean	SD	Mean	SD	Mean	SD	Mean	SD	Mean	SD		Mean	SD
Winter	23-31 December 2008	356.4	7.2	392.2	0.3	-35.8	7.2	15.0	0.9	31.71	0.86	8.05	0.63	1.24	-7.9	2.2
	4-31 December 2009	352.6	9.3	389.4	0.6	-36.8	9.3	15.7	1.1	32.71	0.96	8.24	0.91	1.19	-7.7	4.0
	1-3 January 2006	360.7	17.5	395.4	1.6	-34.7	17.5	12.2	1.1	30.28	4.28	8.12	0.82	1.14	-6.5	6.9
	1-14 January 2009	341.4	2.6	399.3	0.4	-58.0	2.6	8.1	0.8	29.98	0.73	8.42	0.89	1.20	-13.5	1.9
	1-5 January 2010	-	-	-	-	-	-	-	-	-	-	7.95	0.85	1.22	-	-
	1-6 February 2010	329.8	6.6	395.7	0.2	-65.9	6.6	11.3	0.7	32.65	0.45	7.86	0.72	1.21	-13.3	3.8
	1-11 December 2010	384.2	19.7	390.3	0.5	-6.1	19.7	18.0	0.6	33.01	0.65	9.11	0.67	1.23	-1.6	7.5
	Seasonal average	348.2	11.1	394.4	0.9	-46.2	11.1	12.4	1.0	31.47	2.28	8.11	0.89	1.20	-9.8	4.7
Spring	15-31 March 2009	359.4	13.4	391.9	0.4	-32.5	13.5	12.0	0.7	29.89	1.97	7.68	0.93	1.16	-5.8	6.2
	20-30 April 2008	315.6	53.0	396.5	0.7	-81.0	53.0	16.0	1.7	29.99	7.03	5.83	0.41	1.27	-9.9	6.0
	4-30 April 2009	303.5	28.2	395.9	0.3	-92.3	28.2	15.1	0.8	31.21	0.79	5.94	0.42	1.26	-11.5	4.6
	6-10 April 2009	286.3	101.7	398.6	0.7	-112.3	101.7	13.5	1.1	29.83	6.85	5.94	0.42	1.26	-14.0	11.1
	12-15 April 2011	295.8	46.0	398.9	0.4	-103.1	46.0	12.4	0.7	32.42	0.62	6.25	0.31	1.25	-14.0	8.8
	1-20 May 2009	292.7	41.2	388.3	0.4	-95.6	41.2	17.8	0.6	30.28	1.45	5.43	0.26	1.20	-8.9	6.3
	26-31 May 2011	-	-	-	-	-	-	-	-	-	-	5.79	0.23	1.21	-	-
	Seasonal average	308.9	59.9	395.0	0.5	-86.1	59.9	14.5	1.1	30.60	4.55	6.12	0.52	1.23	-10.7	8.2
Summer	1-12 July 2009	357.2	56.0	369.5	0.6	-12.3	56.0	23.3	0.6	30.47	1.18	6.40	0.52	1.18	-1.6	9.3

	2-6 July 2007	292.7	56.1	374.9	0.5	-82.1	56.1	24.5	0.7	30.69	1.50	5.57	0.77	1.27	-8.9	7.3
	6-29 August 2008	339.8	77.9	374.6	0.5	-34.8	77.9	28.0	0.6	31.02	1.16	5.41	0.50	1.21	-3.3	12.6
	17-31 August 2009	293.8	64.5	362.8	0.6	-69.0	64.5	28.6	0.7	30.38	1.52	6.13	0.32	1.22	-8.4	9.7
	1-19 June 2011	302.4	64.6	387.6	0.7	-85.2	64.6	19.7	0.7	32.08	0.76	5.85	0.49	1.27	-10.2	8.0
	Seasonal average	317.2	71.9	373.9	0.6	-56.7	71.9	24.8	0.7	30.93	1.41	5.87	0.60	1.23	-6.5	10.7
Fall	18-25 September 2006	387.8	50.0	374.9	0.7	12.9	50.0	25.3	0.3	33.34	1.08	7.01	0.56	1.19	2.7	5.8
	14-18 October 2006	364.3	65.6	382.8	0.4	-18.5	65.6	25.2	0.4	33.47	1.67	6.12	0.61	1.13	-1.9	5.5
	20-24 November 2006	396.9	23.6	386.3	0.3	10.6	23.6	20.9	0.4	32.93	0.46	7.74	0.69	1.17	1.9	3.7
	1-10 November 2007	395.7	14.4	385.5	0.3	10.3	14.4	22.7	0.3	33.95	0.17	8.14	1.06	1.13	1.9	6.8
	26-30 November 2010	-	-	-	-	-	-	-	-	-	-	6.73	0.74	1.22	-	-
	Seasonal average	393.5	40.4	382.2	0.6	11.3	40.4	23.0	0.5	33.41	0.84	7.41	0.91	1.17	2.2	6.8
Annual average		341.9	59.2	386.4	0.8	-44.4	59.2	18.7	1.0	31.60	3.08	6.88	0.86	1.21	-6.2	9.1

812

813

814

Table 4 Data summary of Domain II. Atm. pCO_2 is atmospheric pCO_2; SST is sea surface temperature; SSS is sea surface salinity; F_{CO2} is the air-sea CO_2 flux, and SD is standard deviation. C_2 is the nonlinearity effect of the short-term variability of wind speeds over a month on the gas transfer velocity, assuming long-term winds followed a Raleigh (Weibull) distribution (Wanninkhof, 1992; Jiang et al., 2008). See text for details. October 2006 and December 2010 were excluded in the calculations of seasonal averages. pCO_2 data are corrected to the reference year 2010.

Season	Period	pCO_2 (μatm)		Atm. pCO_2 (μatm)		ΔpCO_2 (μatm)		SST (℃)		SSS		Wind speed (m s^{-1})		C_2	FCO_2 (mmol m^{-2} d^{-1})	
		Mean	SD	Mean	SD	Mean	SD	Mean	SD	Mean	SD	Mean	SD		Mean	SD
Winter	23-31 December 2008	350.3	8.0	389.0	0.9	-38.6	8.1	16.2	1.7	30.59	1.38	8.56	0.99	1.18	-8.7	1.4
	4-31 December 2009	343.8	7.7	389.8	0.6	-46.1	7.7	19.4	0.7	34.26	0.26	8.02	0.74	1.17	-8.7	0.3
	1-3 January 2006	-	-	-	-	-	-	-	-	-	-	8.71	0.88	1.11	-	-
	1-14 January 2009	347.7	4.5	395.0	0.3	-47.3	4.5	12.7	0.5	29.64	0.47	9.01	1.02	1.12	-10.9	0.9
	1-5 January 2010	353.0	9.3	391.4	1.5	-38.4	9.4	16.6	1.6	32.38	0.91	7.90	0.76	1.22	-7.8	1.9
	1-6 February 2010	352.4	7.2	392.5	0.5	-40.1	7.2	12.7	0.7	31.19	0.49	7.98	0.59	1.20	-8.3	1.6
	1-11 December 2010	-	-	-	-	-	-	-	-	-	-	7.83	0.71	1.28	-	-
	Seasonal average	349.4	8.4	391.5	1.0	-42.1	8.4	15.5	1.3	31.61	0.90	8.36	0.92	1.18	-8.9	1.4
Spring	15-31 March 2009	308.5	13.4	389.6	0.5	-81.1	13.4	18.5	0.8	34.01	0.23	8.30	0.69	1.14	-15.7	2.6
	20-30 April 2008	331.2	22.5	392.0	1.1	-60.9	22.6	21.8	1.7	33.83	0.82	6.38	0.53	1.19	-7.5	3.3
	4-30 April 2009	312.4	11.7	392.1	0.3	-79.7	11.7	20.1	0.2	34.01	0.06	7.00	0.97	1.17	-11.5	1.7
	6-10 April 2009	-	-	-	-	-	-	-	-	-	-	7.00	0.97	1.17	-	-
	12-15 April 2011	-	-	-	-	-	-	-	-	-	-	6.57	0.52	1.24	-	-
	1-20 May 2009	290.6	35.8	386.7	0.7	-96.1	35.8	21.5	1.1	32.63	1.47	5.67	0.56	1.18	-9.4	4.0
	26-31 May 2011	323.1	11.9	394.8	0.9	-71.7	11.9	22.2	0.2	32.63	0.56	6.26	0.42	1.23	-9.1	3.4

	Seasonal average	313.2	23.7	391.1	0.8	-77.9	23.7	20.8	1.1	33.42	0.89	6.74	0.75	1.19	-10.7	3.5
Summer	1-12 July 2009	361.4	16.9	367.1	0.4	-5.7	16.9	26.6	0.3	33.51	0.22	6.33	0.51	1.19	-0.7	2.0
	2-6 July 2007	346.9	11.8	373.5	0.4	-26.6	11.8	26.5	0.8	33.81	0.31	6.86	0.59	1.21	-3.9	1.6
	6-29 August 2008	397.3	2.9	374.7	0.3	22.6	2.9	28.8	0.5	33.40	0.28	5.56	0.40	1.23	2.3	0.3
	17-31 August 2009	363.3	38.0	362.8	0.3	0.5	38.0	28.8	0.3	33.06	0.47	6.19	0.27	1.52	0.1	6.0
	1-19 June 2011	318.6	0.3	387.7	1.6	-69.1	1.6	21.2	0.0	33.40	0.02	6.78	0.43	1.18	-9.5	0.0
	Seasonal average	357.5	21.7	373.2	0.9	-15.7	21.7	26.4	0.5	33.44	0.33	6.34	0.51	1.27	-2.4	3.3
Fall	18-25 September 2006	407.5	14.2	374.8	0.6	32.8	14.2	26.1	0.1	33.04	0.31	7.28	0.77	1.19	5.2	3.0
	14-18 October 2006	308.4	25.3	381.6	0.2	-73.3	25.3	25.7	0.1	33.37	0.43	7.17	1.07	1.12	-10.1	4.7
	20-24 November 2006	377.7	8.1	377.7	8.1	0.0	11.4	23.1	0.3	33.23	0.34	6.97	0.75	1.18	-1.0	1.2
	1-10 November 2007	-	-	-	-	-	-	-	-	-	-	10.81	1.40	1.07	-	-
	26-30 November 2010	378.5	16.4	388.5	0.6	-10.1	16.5	19.5	1.0	32.00	1.40	9.01	1.29	1.10	-2.1	4.8
	Seasonal average	387.9	16.4	380.3	5.7	7.6	17.4	22.9	0.8	32.76	1.05	8.52	1.26	1.13	0.7	4.1
Annual average		352.0	21.4	384.0	3.4	-32.0	21.6	21.4	1.1	32.81	0.97	7.49	1.04	1.19	-5.3	3.7

822 Table 5 Data summary of Domain III. Atm. pCO_2 is atmospheric pCO_2; SST is sea surface temperature; SSS is sea surface salinity; F_{CO2} is the

823 air-sea CO_2 flux, and SD is standard deviation. C_2 is the nonlinearity effect of the short-term variability of wind speeds over a month on the gas

824 transfer velocity, assuming long-term winds followed a Raleigh (Weibull) distribution (Wanninkhof, 1992; Jiang et al., 2008). See text for details.

825 October 2006 and December 2010 were excluded in the calculations of seasonal averages. pCO_2 data are corrected to the reference year 2010.

Season	Period	pCO_2 (μatm)		Atm. pCO_2 (μatm)		ΔpCO_2 (μatm)		SST (℃)		SSS		Wind speed (m s^{-1})		C_2	FCO_2 (mmol m^{-2} d^{-1})	
		Mean	SD	Mean	SD	Mean	SD	Mean	SD	Mean	SD	Mean	SD		Mean	SD
Winter	23-31 December 2008	-	-	-	-	-	-	-	-	-	-	8.21	0.16	1.25	-	-
	4-31 December 2009	340.1	8.8	385.9	0.5	-45.7	8.8	19.6	0.8	34.38	0.15	8.86	0.30	1.18	-10.8	1.4
	1-3 January 2006	-	-	-	-	-	-	-	-	-	-	8.79	0.38	1.13	-	-
	1-14 January 2009	-	-	-	-	-	-	-	-	-	-	9.21	0.25	1.18	-	-
	1-5 January 2010	-	-	-	-	-	-	-	-	-	-	8.48	0.36	1.21	-	-
	1-6 February 2010	-	-	-	-	-	-	-	-	-	-	8.39	0.31	1.19	-	-
	1-11 December 2010	335.2	9.2	387.3	0.5	-52.2	9.2	22.3	0.5	34.42	0.04	9.79	0.51	1.20	-15.3	5.2
	Seasonal average	340.1	8.8	385.9	0.5	-45.7	8.8	19.6	0.8	34.38	0.15	8.66	0.30	1.19	-10.8	1.4
Spring	15-31 March 2009	-	-	-	-	-	-	-	-	-	-	8.81	0.36	1.13	-	-
	20-30 April 2008	-	-	-	-	-	-	-	-	-	-	6.68	0.38	1.21	-	-
	4-30 April 2009	289.5	10.4	396.2	0.8	-106.7	10.4	17.8	1.2	34.14	0.27	6.95	0.62	1.26	-17.8	3.1
	6-10 April 2009	-	-	-	-	-	-	-	-	-	-	6.95	0.62	1.26	-	-
	12-15 April 2011	-	-	-	-	-	-	-	-	-	-	6.93	0.27	1.24	-	-
	1-20 May 2009	-	-	-	-	-	-	-	-	-	-	6.17	0.41	1.20	-	-
	26-31 May 2011	-	-	-	-	-	-	-	-	-	-	5.61	0.25	1.25	-	-

	Seasonal average	289.5	10.4	396.2	0.8	-106.7	10.4	17.8	1.2	34.14	0.27	6.87	0.62	1.22	-17.8	3.1
Summer	1-12 July 2009	-	-	-	-	-	-	-	-	-	-	6.69	0.23	1.14	-	-
	2-6 July 2007	-	-	-	-	-	-	-	-	-	-	5.94	0.61	1.40	-	-
	6-29 August 2008	-	-	-	-	-	-	-	-	-	-	6.23	0.39	1.18	-	-
	17-31 August 2009	378.3	10.2	362.1	0.3	16.2	10.2	29.4	0.3	33.12	0.49	5.59	0.25	1.28	1.8	3.7
	1-19 June 2011	304.0	14.5	386.6	1.2	-82.6	14.5	19.3	0.8	33.34	0.35	6.10	0.65	1.28	-10.9	1.6
	Seasonal average	341.1	17.7	374.3	1.2	-33.2	17.8	24.3	0.9	33.23	0.60	6.11	0.52	1.26	-4.6	4.0
Fall	18-25 September 2006	-	-	-	-	-	-	-	-	-	-	7.08	0.88	1.20	-	-
	14-18 October 2006	-	-	-	-	-	-	-	-	-	-	7.03	0.59	1.14	-	-
	20-24 November 2006	-	-	-	-	-	-	-	-	-	-	7.82	0.52	1.17	-	-
	1-10 November 2007	367.3	8.6	384.9	0.3	-17.6	8.6	23.7	0.3	34.19	0.06	8.96	0.50	1.11	-3.7	5.1
	26-30 November 2010	-	-	-	-	-	-	-	-	-	-	7.40	0.20	1.17	-	-
	Seasonal average	367.3	8.6	384.9	0.3	-17.6	8.6	23.7	0.3	34.19	0.06	7.82	0.50	1.16	-3.7	5.1
Annual average		334.5	13.8	385.3	0.9	-50.8	13.8	21.4	1.0	33.98	0.39	7.36	0.57	1.21	-9.2	4.2

826

827

828

Table 6 Data summary of Domain IV. Atm. pCO_2 is atmospheric pCO_2; SST is sea surface temperature; SSS is sea surface salinity; F_{CO2} is the air-sea CO_2 flux, and SD is standard deviation. C_2 is the nonlinearity effect of the short-term variability of wind speeds over a month on the gas transfer velocity, assuming long-term winds followed a Raleigh (Weibull) distribution (Wanninkhof, 1992; Jiang et al., 2008). See text for details. October 2006 and December 2010 were excluded in the calculations of seasonal averages. pCO_2 data are corrected to the reference year 2010.

Season	Period	pCO_2 (μatm)		Atm. pCO_2 (μatm)		ΔpCO_2 (μatm)		SST (℃)		SSS		Wind speed (m s^{-1})		C_2	FCO_2 (mmol m^{-2} d^{-1})	
		Mean	SD	Mean	SD	Mean	SD	Mean	SD	Mean	SD	Mean	SD		Mean	SD
Winter	23-31 December 2008	335.5	3.8	387.5	0.3	-52.0	3.8	20.6	0.6	34.04	0.32	8.85	0.34	1.16	-11.8	0.9
	4-31 December 2009	339.1	5.1	387.3	0.7	-48.2	5.1	20.1	0.8	34.55	0.08	8.60	0.19	1.19	-10.8	1.6
	1-3 January 2006	-	-	-	-	-	-	-	-	-	-	9.02	0.30	1.11	-	-
	1-14 January 2009	-	-	-	-	-	-	-	-	-	-	9.36	0.45	1.16	-	-
	1-5 January 2010	347.5	2.3	389.3	0.2	-41.8	2.3	19.1	0.3	34.46	0.12	8.42	0.30	1.19	-9.0	0.5
	1-6 February 2010	-	-	-	-	-	-	-	-	-	-	9.06	0.14	1.16	-	-
	1-11 December 2010	331.2	4.0	388.7	0.5	-57.5	4.1	22.6	0.5	34.46	0.04	8.96	0.17	1.22	-14.6	1.3
	Seasonal average	340.7	4.8	388.0	0.6	-47.3	4.8	19.9	0.8	34.35	0.25	8.89	0.33	1.17	-10.6	1.3
Spring	15-31 March 2009	305.8	13.5	387.6	0.7	-81.8	13.5	21.3	1.0	34.36	0.10	9.15	0.20	1.13	-18.7	3.1
	20-30 April 2008	-	-	-	-	-	-	-	-	-	-	7.07	0.21	1.17	-	-
	4-30 April 2009	326.3	16.0	391.6	0.8	-65.4	16.1	21.5	1.3	33.99	0.52	7.57	0.37	1.15	-10.6	0.7
	6-10 April 2009	-	-	-	-	-	-	-	-	-	-	7.57	0.37	1.15	-	-
	12-15 April 2011	317.3	17.5	396.3	1.0	-79.0	17.6	18.4	1.5	34.43	0.34	6.88	0.08	1.18	-11.3	0.9
	1-20 May 2009	300.1	20.1	388.6	0.8	-88.6	20.1	21.0	1.3	33.81	0.44	5.98	0.22	1.16	-9.2	2.8
	26-31 May 2011	342.8	7.3	394.0	0.1	-51.3	7.3	22.7	0.4	34.24	0.18	6.17	0.35	1.21	-6.1	0.6

	Seasonal average	318.4	17.3	391.6	0.8	-73.2	17.4	21.0	1.3	34.17	0.39	7.20	0.30	1.16	-11.2	2.2
Summer	1-12 July 2009	388.7	5.0	366.7	0.2	22.0	5.0	27.1	0.3	33.95	0.14	6.75	0.12	1.14	2.8	0.6
	2-6 July 2007	375.0	12.5	372.9	0.2	2.1	12.5	28.2	0.3	33.76	0.12	6.95	0.25	1.27	0.4	2.1
	6-29 August 2008	392.7	2.4	374.7	0.2	18.1	2.4	28.7	0.2	33.48	0.17	5.51	0.16	1.18	1.6	0.2
	17-31 August 2009	400.4	5.8	361.0	0.3	39.4	5.8	29.5	0.3	33.66	0.13	6.05	0.23	1.47	6.7	2.1
	1-19 June 2011	345.1	9.8	386.6	1.2	-41.5	9.9	22.9	0.7	34.18	0.25	7.33	0.24	1.17	-6.5	0.2
	Seasonal average	380.4	8.9	372.4	0.6	8.0	8.9	27.3	0.4	33.81	0.19	6.52	0.23	1.25	1.0	1.5
Fall	18-25 September 2006	-	-	-	-	-	-	-	-	-	-	6.39	0.42	1.26	-	-
	14-18 October 2006	327.6	35.5	381.8	0.2	-54.2	35.5	25.7	0.3	34.18	0.33	7.56	0.28	1.10	-7.9	0.1
	20-24 November 2006	-	-	-	-	-	-	-	-	-	-	7.06	0.14	1.18	-	-
	1-10 November 2007	-	-	-	-	-	-	-	-	-	-	10.37	0.53	1.08	-	-
	26-30 November 2010	336.4	2.4	386.8	0.3	-50.4	2.4	21.8	0.2	34.42	0.04	8.39	0.40	1.11	-9.3	0.5
	Seasonal average	336.4	2.4	386.8	0.3	-50.4	2.4	21.8	0.2	34.42	0.04	8.05	0.40	1.15	-9.3	0.5
Annual average		344.0	11.7	384.7	0.7	-40.7	11.7	22.5	0.9	34.18	0.29	7.66	0.37	1.18	-7.5	1.7

833

834

835

836 Table 7 Data summary of Domain V. Atm. pCO_2 is atmospheric pCO_2; SST is sea surface temperature; SSS is sea surface salinity; F_{CO2} is the

837 air-sea CO_2 flux, and SD is standard deviation. C_2 is the nonlinearity effect of the short-term variability of wind speeds over a month on the gas

838 transfer velocity, assuming long-term winds followed a Raleigh (Weibull) distribution (Wanninkhof, 1992; Jiang et al., 2008). See text for details.

839 October 2006 and December 2010 were excluded in the calculations of seasonal averages. pCO_2 data are corrected to the reference year 2010.

Season	Period	pCO_2 (μatm)		Atm pCO_2 (μatm)		ΔpCO_2 (μatm)		SST (℃)		SSS		Wind speed (m s^{-1})		C_2	FCO_2 (mmol m^{-2} d^{-1})	
		Mean	SD	Mean	SD	Mean	SD	Mean	SD	Mean	SD	Mean	SD	Mean	Mean	SD
Winter	23-31 December 2008	340.5	4.3	386.5	0.5	-46.0	4.36	21.2	0.9	34.00	0.17	9.21	0.52	1.14	-10.9	1.0
	4-31 December 2009	340.8	2.9	387.3	0.3	-46.5	2.92	23.1	0.3	34.66	0.06	8.74	0.44	1.16	-10.2	2.4
	1-3 January 2006	-	-	-	-	-	-	-	-	-	-	9.30	0.46	1.11	-	-
	1-14 January 2009	-	-	-	-	-	-	-	-	-	-	10.02	0.49	1.09	-	-
	1-5 January 2010	349.6	11.2	389.3	0.2	-39.7	11.21	21.0	1.1	34.58	0.04	8.78	0.50	1.17	-9.0	2.5
	1-6 February 2010	-	-	-	-	-	-	-	-	-	-	8.39	0.80	1.20	-	-
	1-11 December 2010	-	-	-	-	-	-	-	-	-	-	8.41	0.49	1.24	-	-
	Seasonal average	343.6	8.7	387.7	0.5	-44.1	8.75	21.7	1.0	34.41	0.13	9.07	0.60	1.16	-10.0	2.5
Spring	15-31 March 2009	326.5	20.6	386.7	1.0	-60.3	20.61	24.2	1.8	34.21	0.09	8.82	0.56	1.12	-12.5	4.3
	20-30 April 2008	-	-	-	-	-	-	-	-	-	-	6.96	0.47	1.17	-	-
	4-30 April 2009	354.9	6.4	387.8	1.6	-32.9	6.59	24.9	2.2	34.32	0.06	8.03	0.32	1.12	-5.6	1.1
	6-10 April 2009	-	-	-	-	-	-	-	-	-	-	8.03	0.32	1.12	-	-
	12-15 April 2011	339.8	7.0	392.5	1.0	-52.7	7.08	24.1	0.8	34.70	0.06	6.88	0.33	1.17	-7.2	-7.2
	1-20 May 2009	342.8	7.6	385.3	0.9	-42.5	7.70	24.0	1.2	34.27	0.08	6.09	0.27	1.14	-4.4	0.9
	26-31 May 2011	362.0	6.0	394.0	0.1	-32.1	6.04	24.6	0.7	34.22	0.11	6.46	0.33	1.21	-4.2	0.4

	Seasonal average	345.2	12.3	389.3	1.2	-44.1	12.39	24.4	1.6	34.34	0.09	7.32	0.41	1.15	-6.8	4.3
Summer	1-12 July 2009	380.5	12.9	366.5	0.5	14.0	12.96	27.6	1.0	34.00	0.20	6.52	0.43	1.23	1.9	0.2
	2-6 July 2007	388.5	11.6	373.9	1.6	14.7	11.67	28.4	1.8	34.18	0.28	6.14	0.64	1.26	1.9	0.2
	6-29 August 2008	374.3	10.2	374.4	0.4	-0.1	10.23	28.6	0.4	33.05	0.33	5.33	0.31	1.24	-0.0	0.2
	17-31 August 2009	378.8	19.8	363.7	0.7	15.0	19.80	28.1	0.7	33.53	0.22	5.91	0.43	1.70	3.2	4.8
	1-19 June 2011	-	-	-	-	-	-	-	-	-	-	6.90	0.55	1.19	-	-
	Seasonal average	380.5	16.3	369.6	1.1	10.9	16.34	28.2	1.3	33.69	0.30	6.16	0.54	1.32	1.8	2.8
Fall	18-25 September 2006	-	-	-	-	-	-	-	-	-	-	6.93	0.60	1.19	-	-
	14-18 October 2006	-	-	-	-	-	-	-	-	-	-	7.80	0.52	1.09	-	-
	20-24 November 2006	-	-	-	-	-	-	-	-	-	-	7.27	0.38	1.16	-	-
	1-10 November 2007	-	-	-	-	-	-	-	-	-	-	11.42	0.66	1.06	-	-
	26-30 November 2010	347.9	6.1	385.9	0.6	-38.1	6.16	24.6	0.8	34.43	0.07	9.46	0.75	1.08	-8.4	2.0
	Seasonal average	347.9	6.1	385.9	0.6	-38.1	6.16	24.6	0.8	34.43	0.07	8.77	0.75	1.12	-8.4	2.0
Annual average		354.3	13.3	383.1	1.0	-28.8	13.35	24.7	1.4	34.22	0.20	7.83	0.68	1.19	-5.9	3.4

840
841
842

843 Table 8 Comparison of air-sea CO_2 fluxes in the East China Sea shelf

844

Study area	Season	Methods*	Wind speed	k [§]	FCO_2 (mmol m^{-2} d^{-1})	$FCO_2\_S(07)$ [#] (mmol m^{-2} d^{-1})	Data source
Domain I	Spring	1	Short-term	W92_S	-8.8±5.8	-7.7±5.1	Zhai and Dai (2009)
	Spring	1	Monthly	S07		-10.7±8.2	This study
	Summer	1	Short-term	W92_S	-4.9±4.0	-4.3±3.5	Zhai and Dai (2009)
	Summer	1	Monthly	S07		-6.5±10.7	This study
	Fall	1	Short-term	W92_S	2.9±2.5	2.5±2.2	Zhai and Dai (2009)
	Fall	1	Monthly	S07		2.2±6.8	This study
	Winter	1	Short-term	W92_S	-10.4±2.3	-9.1±2.0	Zhai and Dai (2009)
	Winter	1	Monthly	S07		-9.8±4.6	This study
	Annual	1	Short-term	W92_S	-5.2±3.6	-4.5±3.1	Zhai and Dai (2009)
	Annual	1	Monthly	S07		-6.2±9.1	This study
Domains I and III	Spring	1	Monthly	W92_L	-5.0±1.6	-4.2±1.3	Shim et al. (2007)
	Spring	1	Daily	W92_S	-6.8±4.3	-5.9±3.7	Kim et al. (2013)
	Spring	1	Monthly	S07		-13.0±6.6	This study
	Summer	1	Daily	W92_S	-6.6±8.5	-5.7±7.4	Kim et al. (2013)
	Summer	1	Monthly	S07		-5.8±8.5	This study
	Fall	1	Monthly	W92_L	1.1±2.9	0.9±2.4	Shim et al. (2007)
	Fall	1	Daily	W92_S	0.8±7.3	0.7±6.4	Kim et al. (2013)
	Fall	1	Monthly	S07		0.2±6.2	This study

	Winter	1	Daily	W92_S	-12±4.1	-10.5±3.6	Kim et al. (2013)
	Winter	1	Monthly	S07		-10.1±3.6	This study
	Annual	4	-	-	-8	-	Tsunogai et al. (1999)
	Annual	1	Daily	W92_S	-6.0±5.8	-5.2±5.0	Kim et al. (2013)
	Annual	1	Monthly	S07		-7.2±6.2	This study
Domains I, III and IV	Summer	2	-	L&M86; T90	-1.8 to -4.8	-	Wang et al. (2000)
	Summer	1	Monthly	S07		-4.6±5.9	This study
Domains II, IV and V	Spring	2	Long-term	-	-5.8±7.7	-	Peng et al. (1999)
	Spring	1	Monthly	S07		-9.5±2.0	This study
ECS shelf	Spring	3	Monthly	S07	-	-8.2±2.1	Tseng et al. (2014)
	Spring	3	Long-term	W92_L	-11.5±2.5	-9.6±2.1	Tseng et al. (2011)
	Spring	1	Monthly	S07		-11.7±3.6	This study
	Summer	1	Daily	S07		-2.4±3.1	Chou et al. (2009)
	Summer	3	Long-term	W92_L	-1.9±1.4	-1.6±1.2	Tseng et al. (2011)
	Summer	3	Monthly	S07		-2.5±3.0	Tseng et al. (2014)
	Summer	1	Monthly	S07		-3.5±4.6	This study
	Fall	3	Long-term	W92_L	-2.2±3.0	-1.8±2.5	Tseng et al. (2011)
	Fall		Monthly	S07		-0.8±1.9	Tseng et al. (2014)
	Fall	1	Monthly	S07		-2.3±3.1	This study
	Winter	1	Monthly	W92_L	-13.7±5.7	-11.4±4.7	Chou et al. (2011)
	Winter	3	Long-term	W92_L	-9.3±1.9	-7.7±1.6	Tseng et al. (2011)
	Winter	3	Monthly	S07		-5.5±1.6	Tseng et al. (2014)
	Winter	1	Monthly	S07		-10.0±2.0	This study

	Annual	3	Long-term	W92_L	-6.3±1.1	-5.2±0.9	Tseng et al. (2011)
	Annual	3	Monthly	S07		-3.8±1.1	Tseng et al. (2014)
	Annual	1	Monthly	S07		-6.9±4.0	This study

* Methods

1: pCO_2 measurements and gas transfer algorithms with wind speeds;

2: pCO_2 calculated from DIC and TA and gas transfer algorithms with wind speeds;

3: pCO_2 algorithms (with Changjiang discharge and SST) and gas transfer algorithms with wind speeds;

4: pCO_2 measurements and algorithms (with SST, SSS and phosphate) and given gas transfer velocity;

§: W92_S is Wanninkhof (1992) algorithm for short-term wind speeds; W92_L is Wanninkhof (1992) algorithm for long-term (or monthly average) wind speeds; S07 is Sweeney et al. (2007) algorithm; L&M86 is Liss and Merlivat (1986) algorithm; T90 is Tans (1990) algorithm.

#: FCO_2 data were calculated (or recalculated) with the Sweeney et al. (2007) gas transfer algorithm with wind speed.

859 Figure captions

860 Fig. 1 Map of the East China Sea showing the study area. Areas framed with black
861 solid lines indicate the five physico-biogeochemical domains categorized in this study
862 to better constrain the spatial and temporal variability of CO_2 fluxes, as detailed in
863 Table 1. The arrows show the direction of the Kuroshio Current. The area framed by
864 pink dashed lines shows the study area of Shim et al. (2007) and Kim et al. (2013); by
865 brown dashed lines of Zhai and Dai (2009); by blue dashed lines of Wang et al. (2000);
866 by red dashed lines of Chou et al. (2009a; 2011) and Tseng et al. (2011); and by black
867 dashed lines of Peng et al. (1999). The solid brown line is the PN line which was the
868 major survey track of Tsunogai et al. (1999). Note that the color bar for the depth
869 scale is non-linear.

870 Fig. 2 Spatial distribution of surface water pCO_2 (μatm) in the East China Sea in the
871 12 month surveys of 2006 to 2011. The framed areas show the five
872 physico-biogeochemical domains. Data are corrected to the reference year 2010.

873 Fig. 3 Spatial distribution of sea surface temperature (SST) in the East China Sea in
874 the 12 month surveys of 2006 to 2011. The climatology (from 2003 to 2013)
875 monthly-mean SST were calculated based on the monthly mean SST obtained from
876 the NASA ocean color website (http://oceancolor.gsfc.nasa.gov), which were retrieved
877 with the Moderate Resolution Imaging Spectroradiometer (MODIS) on board the
878 Aqua satellite. The 4 μm nighttime SST products were used here. The SST data in the
879 track were measured during the surveys. The framed areas show the five
880 physico-biogeochemical domains. In panel M, the SST data in the track were
881 measured during the December 2010 cruise while the background is the climatology
882 (from 2003 to 2013) monthly-mean SST.

883 Fig. 4 Seasonal variations of sea surface temperature (SST, A) and salinity (SSS, B) in
884 Domain I (red curve), Domain II (blue curve), Domain III (pink curve), Domain IV
885 (green curve) and Domain V (black curve). The mean SST data were retrieved with
886 the Moderate Resolution Imaging Spectroradiometer (MODIS) on board the Aqua

887 satellite from NASA ocean color website (http://oceancolor.gsfc.nasa.gov). The 4 μm
888 nighttime SST products were used here. The mean SSS were based on the data
889 presented in Tables 3-7. The data during each survey are shown as mean±standard
890 deviation.

891 Fig. 5 Temporal distribution of atmospheric CO_2 concentrations based on ship-board
892 measurements during the cruise to the East China Sea (arithmetic average, red solid
893 dots) and its comparison with the measurements at 21 m above sea level, at Tae-ahn
894 Peninsula (blue solid line) (36.7376 °N, 126.1328 °E, Republic of Korea,
895 http://www.esrl.noaa.gov/gmd/dv/site) and at Mauna Loa Observatory at Hawaii (pink
896 solid line, Scripps CO_2 program, http://scrippsco2.ucsd.edu. The error bars are the
897 standard deviations. The CO_2 concentrations in this plot are the original values in the
898 year of the observations.

899 Fig. 6 Distribution of seasonal average and standard deviations (SD) of pCO_2 in 1°×1°
900 grids on the East China Sea shelf. The framed areas show the five
901 physico-biogeochemical domains. Panel A-1 and A-2 are the result of the winter
902 cruises excluding December 2010; panels D-1 and D-2 are results of the fall cruises
903 excluding October 2006. Data are corrected to the reference year 2010. The surveys
904 conducted in October 2006 and November 2010 were not excluded in the seasonal
905 average calculations and were presented separately, which was due mainly to the
906 abnormal characters of these two surveys. See detail in the text.

907 Fig. 7 CO_2 fluxes and seasonal variations in the East China Sea. The error bars are the
908 standard deviations.

909 Fig. 8 Relationships of pCO_2 and $NpCO_2$ (normalized pCO_2 to 21 °C) of the surface
910 water with sea surface temperature (SST). Panels A-1 and B-1 are Domain I; panels
911 A-2 and B-2 are Domain II; panels A-3 and B-3 are Domain III; panels A-4 and B-4
912 are Domain IV; panels A-5 and B-5 are Domain V. The dashed lines in panels A-1 to
913 A-5 represent $250\times\exp((SST-21)\times0.0423)$ and $400\times\exp((SST-21)\times0.0423)$ μatm, in
914 which 250 and 400 μatm are the lower and higher limits of $NpCO_2$ in Domains IV and

915 V (see details in the text). pCO_2 and NpCO_2 values are in the year of observations.

916 Fig. 9 Relationships of pCO_2 of the surface water with sea surface salinity (SSS).
917 Panels A, B, C, D and E are Domains I to V, respectively. pCO_2 values are in the year
918 of observations.

919 Fig. 10 Relationships of pCO_2 and NpCO_2 (normalized pCO_2 to 21 ℃) with
920 chlorophyll a (Chl-*a*) concentration. The data of Chl-*a* concentration in surface water
921 were unpublished data from Dr. Jun Sun. The spring surveys include April and May
922 2011; the summer surveys include July and August 2009; the fall surveys include
923 November 2010; and the winter surveys include December 2009 and January 2010
924 surveys. Panels A-1 and B-1 are Domain I; panels A-2 and B-2 are Domain II; panels
925 A-3 and B-3 are Domain III; panels A-4 and B-4 are Domain IV; panels A-5 and B-5
926 are Domain V. pCO_2 and NpCO_2 values are in the year of observations.

927

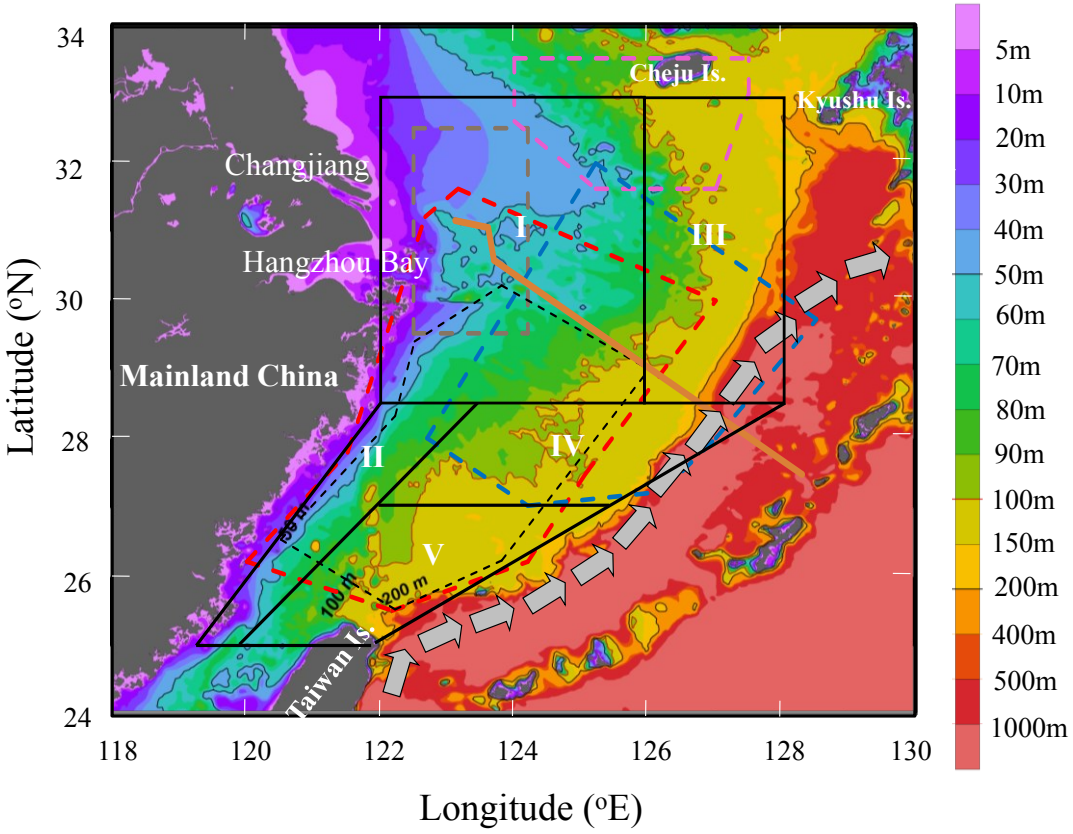
Cheju Is.
Kyushu Is.
Changjiang
Hangzhou Bay
Mainland China
I
II
III
IV
V
50 m
100 m
200 m
Taiwan Is.
34
32
30
28
26
24
118
120
122
124
126
128
130
Latitude (°N)
Longitude (°E)
5m
10m
20m
30m
40m
50m
60m
70m
80m
90m
100m
150m
200m
400m
500m
1000m

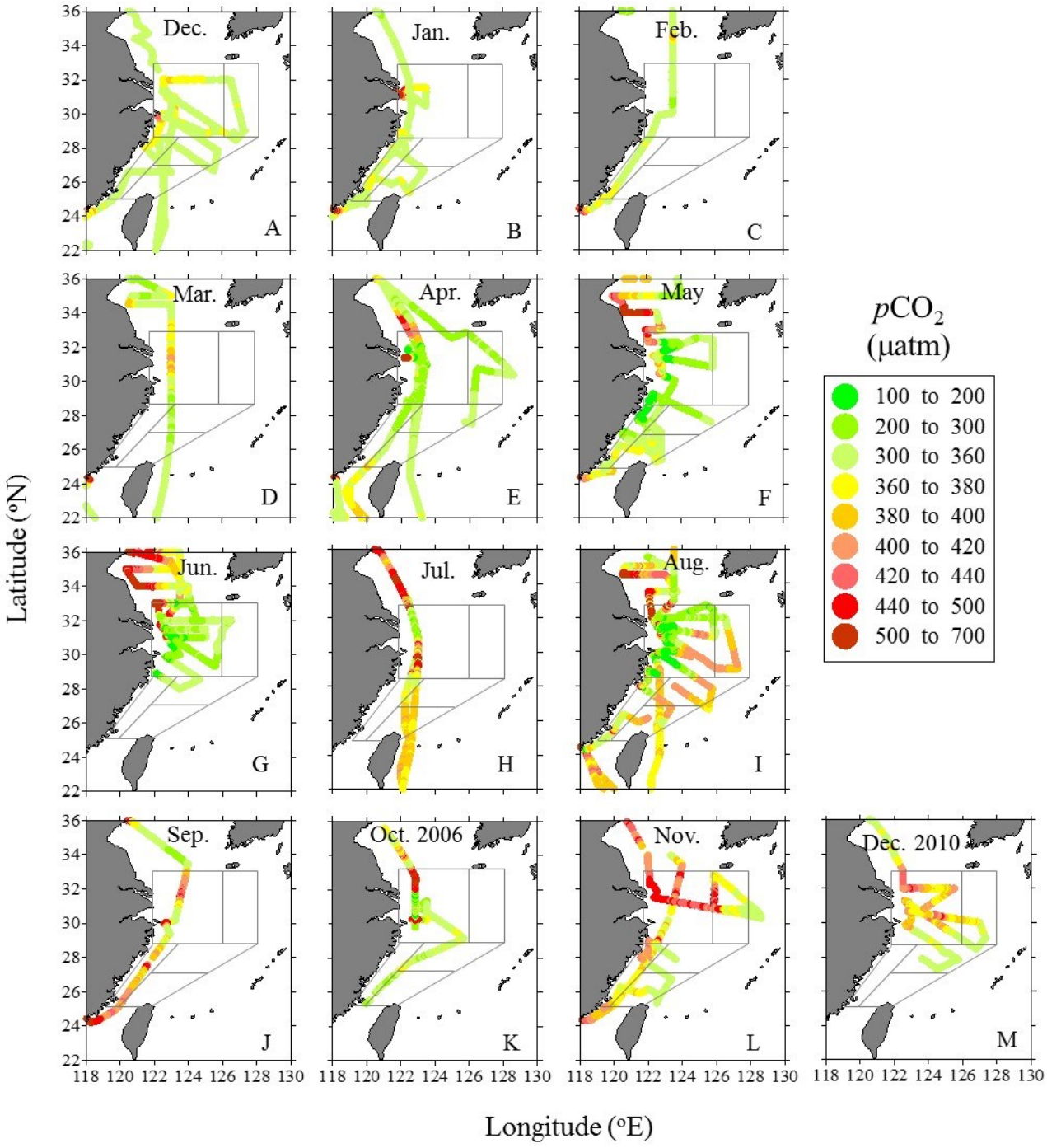
Dec.
Jan.
Feb.
Mar.
Apr.
May
Jun.
Jul.
Aug.
Sep.
Oct. 2006
Nov.
Dec. 2010
A
B
C
D
E
F
G
H
I
J
K
L
M
pCO_2 (μatm)
100 to 200
200 to 300
300 to 360
360 to 380
380 to 400
400 to 420
420 to 440
440 to 500
500 to 700
Latitude (°N)
Longitude (°E)
22 24 26 28 30 32 34 36
118 120 122 124 126 128 130

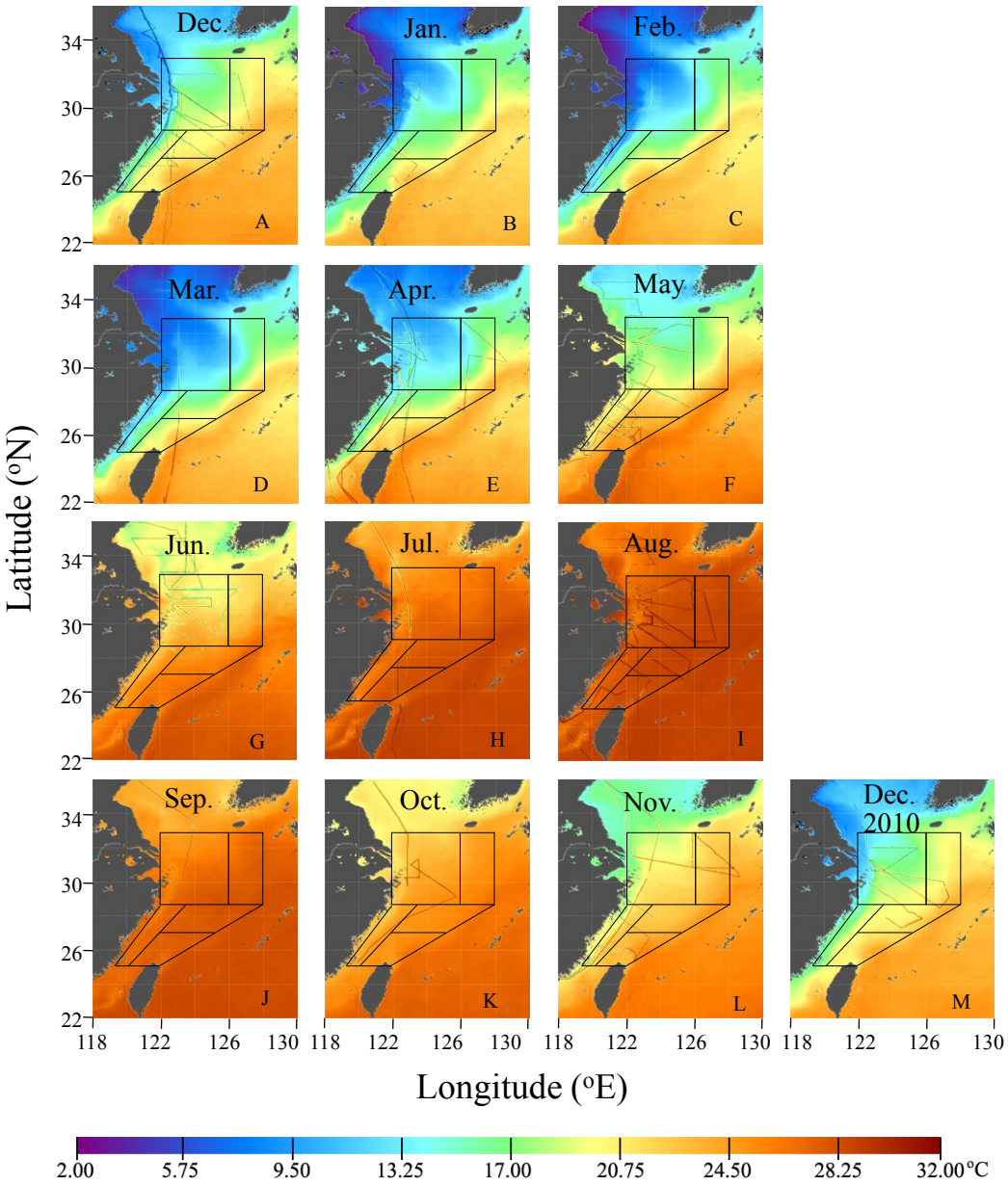
Dec.
A
Jan.
B
Feb.
C
Mar.
D
Apr.
E
May
F
Jun.
G
Jul.
H
Aug.
I
Sep.
J
Oct.
K
Nov.
L
Dec.
2010
M
Latitude (°N)
34
30
26
22
118
122
126
130
Longitude (°E)
2.00
5.75
9.50
13.25
17.00
20.75
24.50
28.25
32.00 °C

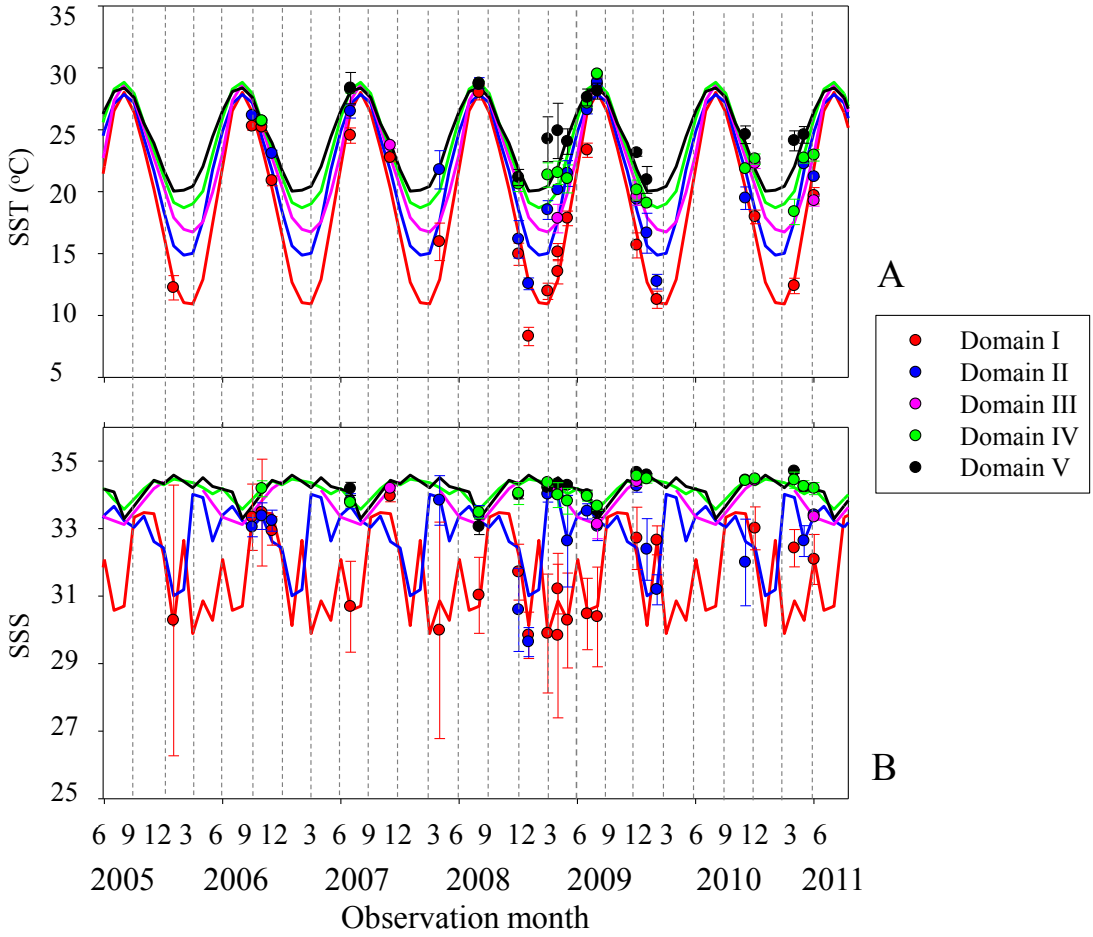
SST (°C)
35
30
25
20
15
10
5
A
Domain I
Domain II
Domain III
Domain IV
Domain V
SSS
35
33
31
29
27
25
B
6 9 12 3 6 9 12 3 6 9 12 3 6 9 12 3 6 9 12 3 6 9 12 3 6
2005 2006 2007 2008 2009 2010 2011
Observation month

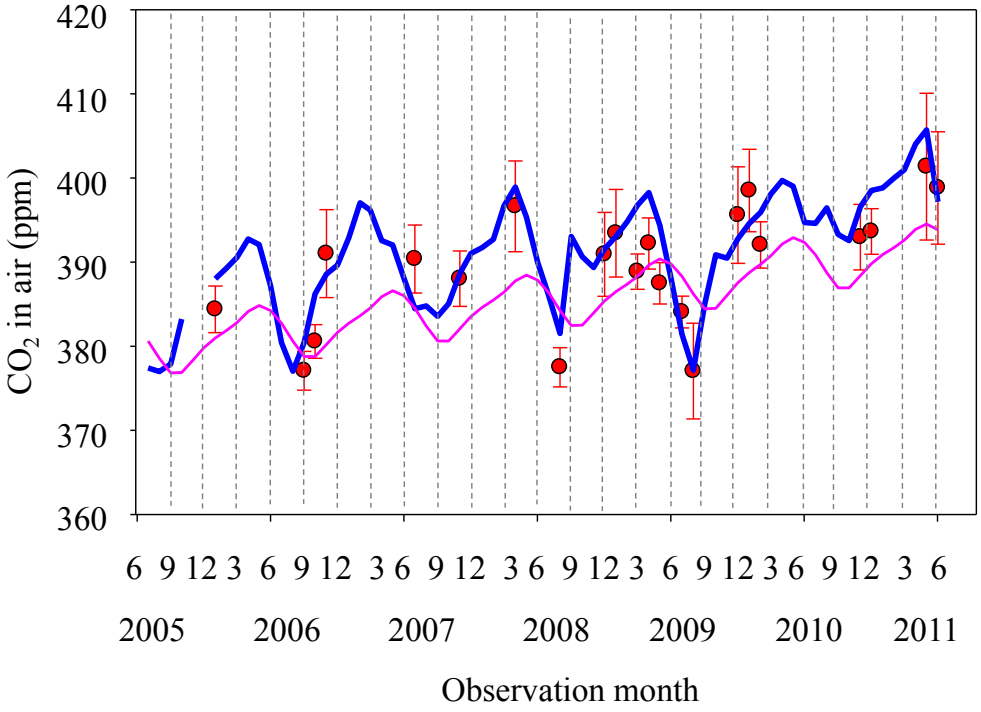
420
410
400
390
380
370
360
CO_2 in air (ppm)
6 9 12 3 6 9 12 3 6 9 12 3 6 9 12 3 6 9 12 3 6 9 12 3 6
2005
2006
2007
2008
2009
2010
2011
Observation month

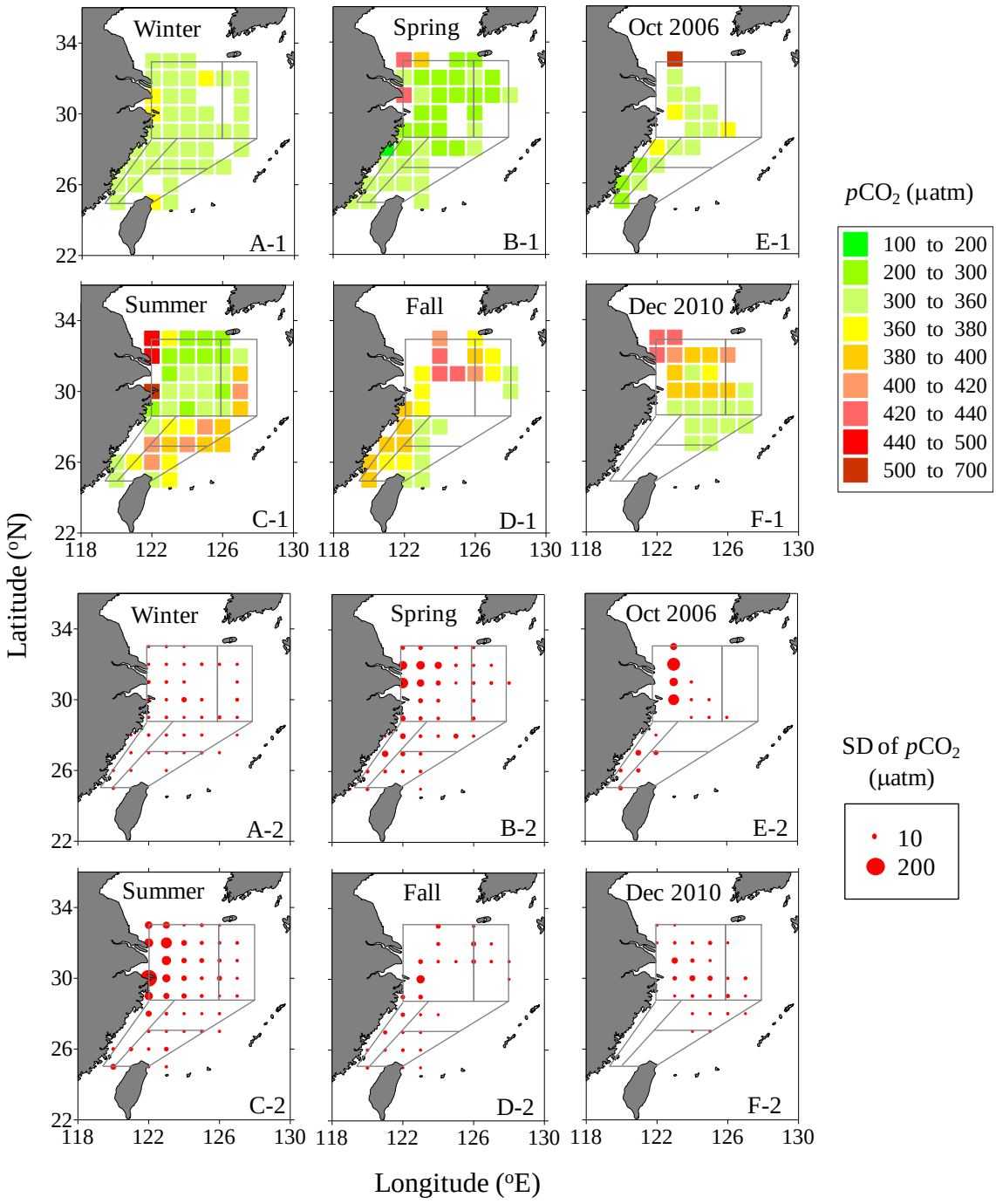
Winter
Spring
Oct 2006
A-1
B-1
E-1
Summer
Fall
Dec 2010
C-1
D-1
F-1
A-2
B-2
E-2
C-2
D-2
F-2
34
30
26
22
118
122
126
130
Latitude (°N)
Longitude (°E)
pCO2 (µatm)
100 to 200
200 to 300
300 to 360
360 to 380
380 to 400
400 to 420
420 to 440
440 to 500
500 to 700
SD of pCO2 (µatm)
10
200

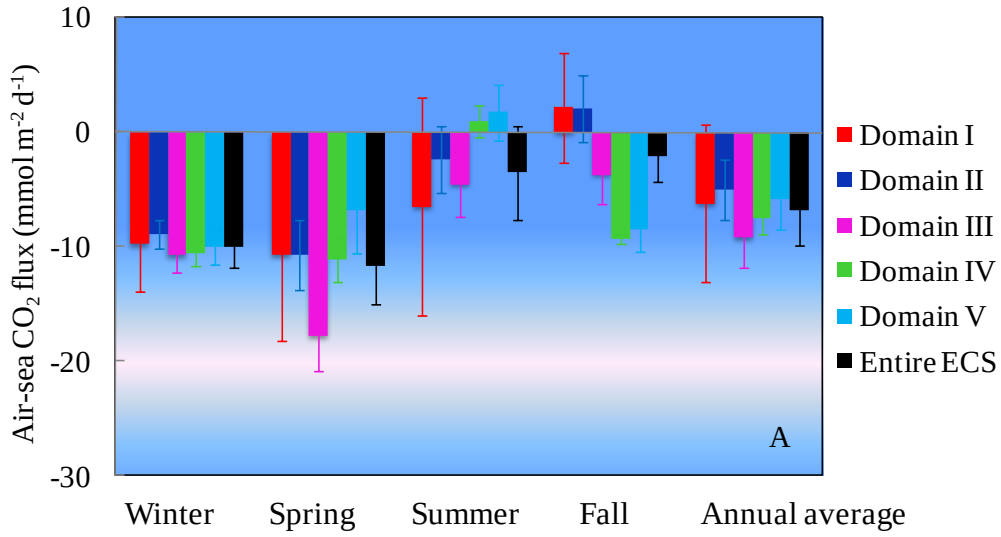
10
0
-10
-20
-30
Air-sea CO_2 flux (mmol m^{-2} d^{-1})
A
Domain I
Domain II
Domain III
Domain IV
Domain V
Entire ECS
Winter
Spring
Summer
Fall
Annual average

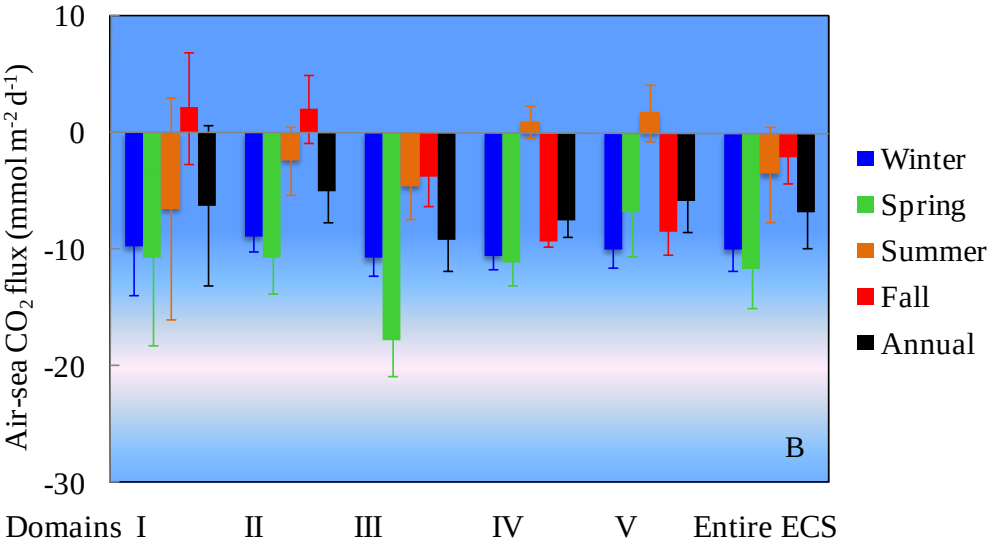
10
0
-10
-20
-30
Air-sea CO_2 flux (mmol m^{-2} d^{-1})
B
Winter
Spring
Summer
Fall
Annual
Domains I
II
III
IV
V
Entire ECS

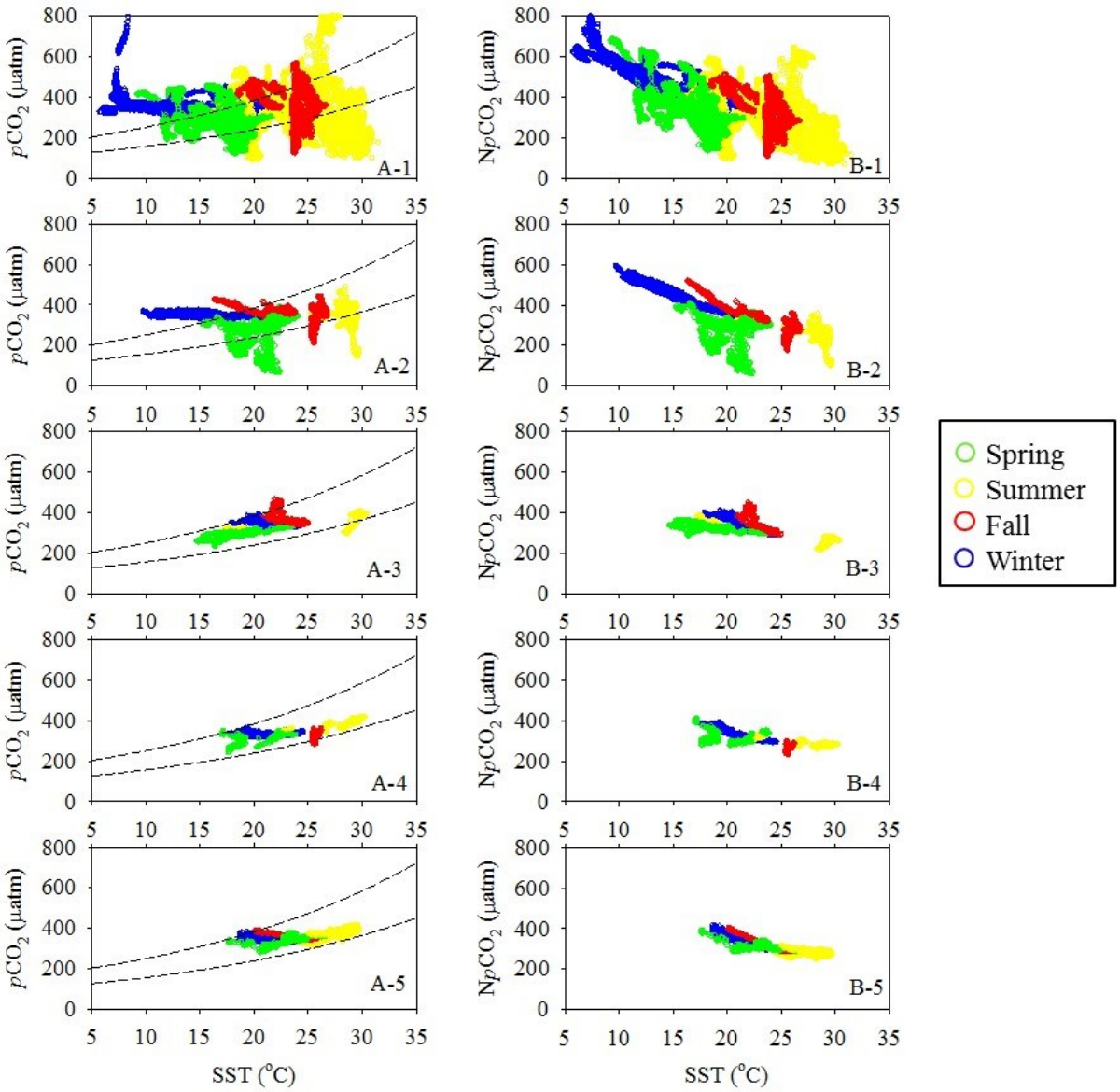
A-1
A-2
A-3
A-4
A-5
B-1
B-2
B-3
B-4
B-5
pCO2 (μatm)
NpCO2 (μatm)
SST (°C)
Spring
Summer
Fall
Winter

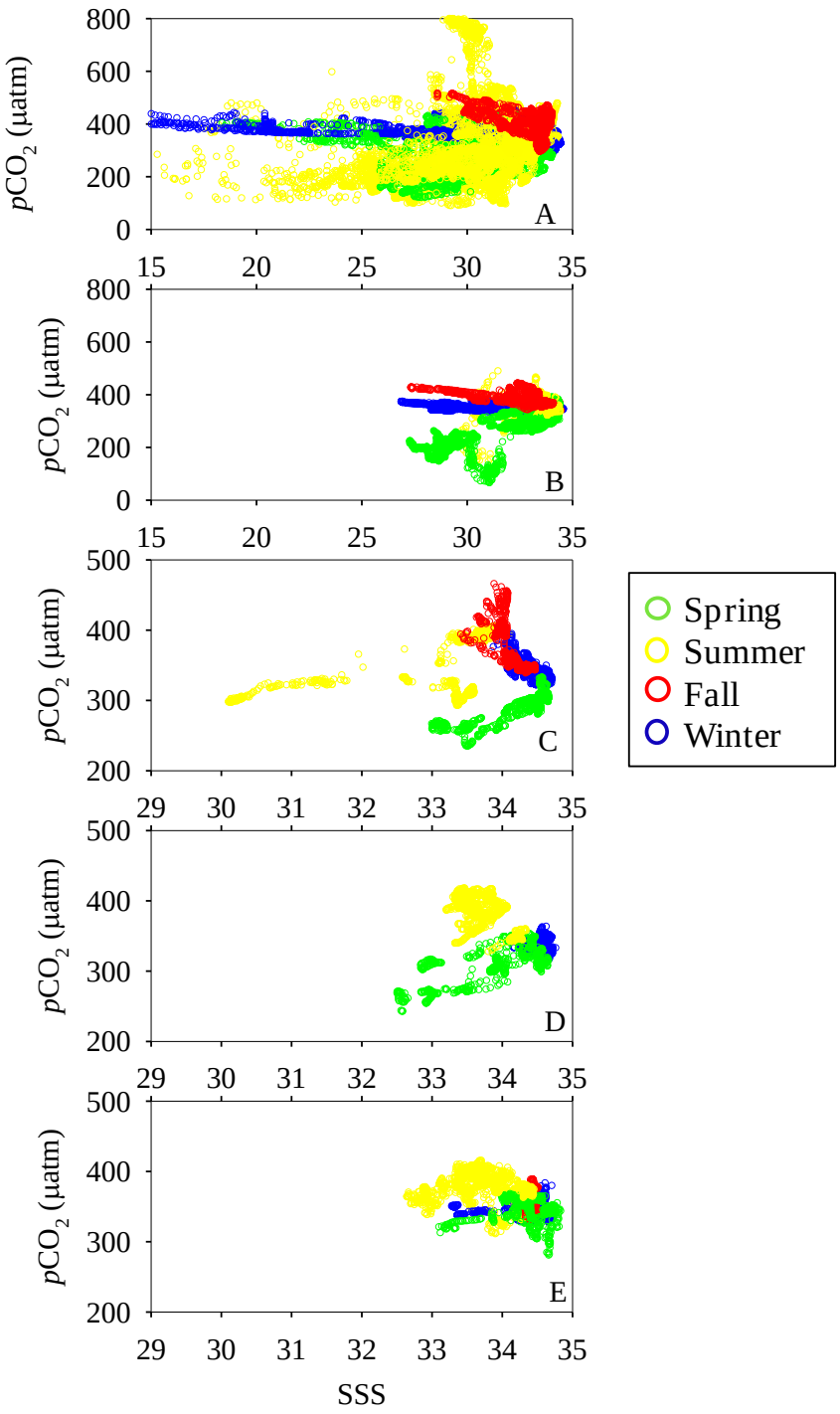
pCO2 (µatm)
800
600
400
200
0
A
15
20
25
30
35
B
500
300
C
29
31
32
33
34
D
E
SSS
Spring
Summer
Fall
Winter

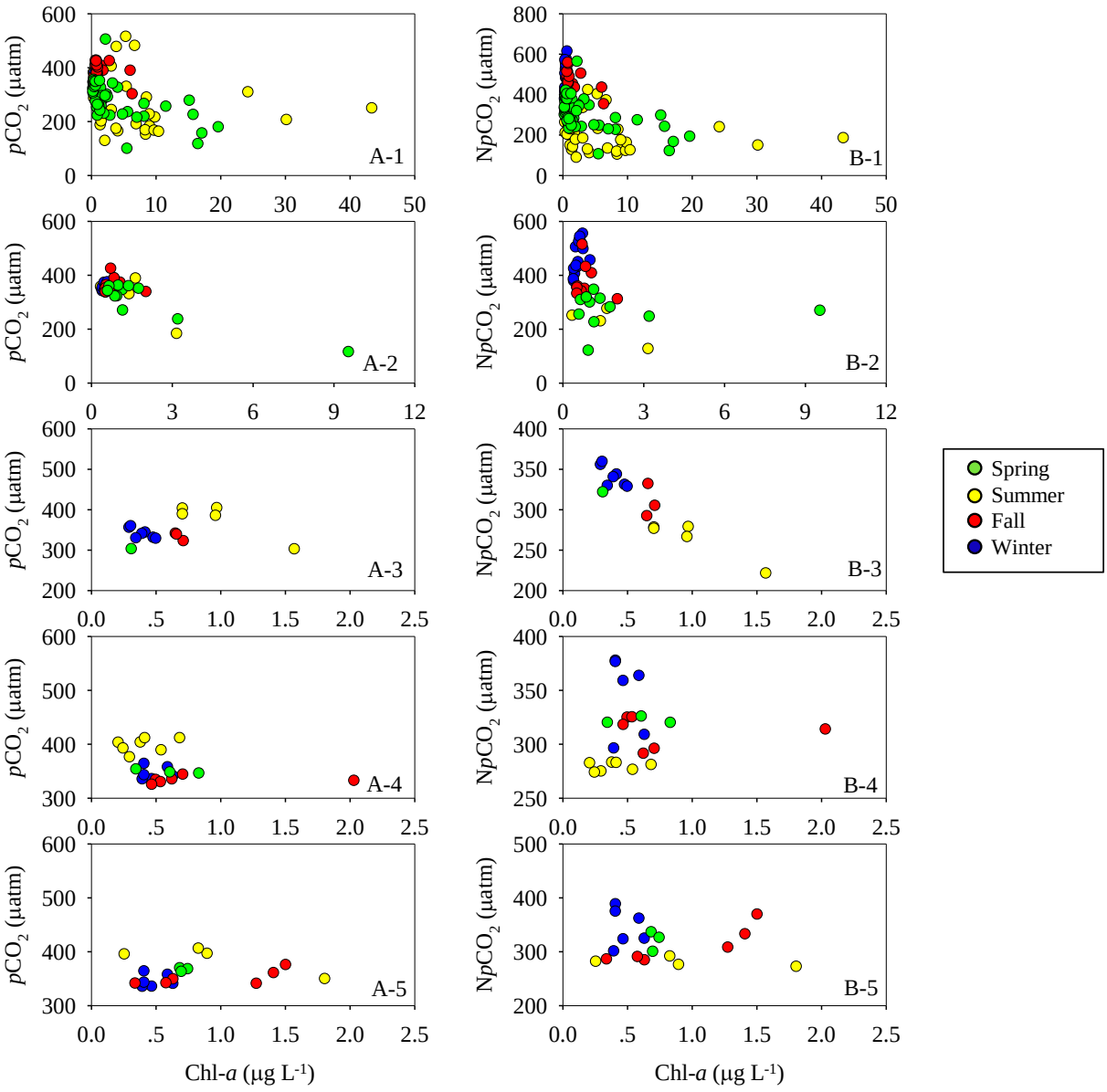
pCO2 (µatm)
NpCO2 (µatm)
A-1
B-1
A-2
B-2
A-3
B-3
A-4
B-4
A-5
B-5
Chl-a (µg L-1)
Spring
Summer
Fall
Winter